Chapter 1

Background of adaptive modulation

Some fundamental concepts are introduced in this chapter such that the adaptive modulation theory and simulation result in the following chapters can be understood more accurately.

1.1 Wireless communication channel

In wireless communication, the transmitted radio frequency (RF) signals experiencing reflection, diffraction, and scattering may take many different routes between the transmitted and the receiver. The multi-path components of the transmitted signal arrive at the receiver with different amplitude, phase, and delay time [1]. Each path of the impulse response experiences different fading effect. The fading results from the constructively or destructively adding of the multi-path components for the path. If there is only one main path, the channel is flat fading channel and no ISI (inter-symbol interference) exists. If there is more than one path in the impulse response, ISI is inevitable and the channel is called frequency selective fading channel because the frequency response of the channel is not constant over the entire spectrum.

If there is no line-of-sight (LOS) component among the multi-path signals, the received signal is often modeled as Rayleigh fading. In this case, the amplitude of the received signal's envelope is Rayleigh distributed and the received instantaneous signal to noise ratio (iSNR) is exponentially distributed.

The fading effect makes no fix-mode modulation scheme work well even with a large SNR margin. Let's take flat fading as an example. In fig. 1.1 and 1.2 the BER of various modulation schemes over AWGN channel and flat fading channel are shown. It's clear that performance of fix-mode modulation scheme degrades very much in fading channel environment. For frequency-selective fading channel the problem is even more serious since the imperfect equalization effect will make the BER performance degrades more. Adaptive modulation is one of the useful techniques counteracting the fading effect and is introduced in the next section.
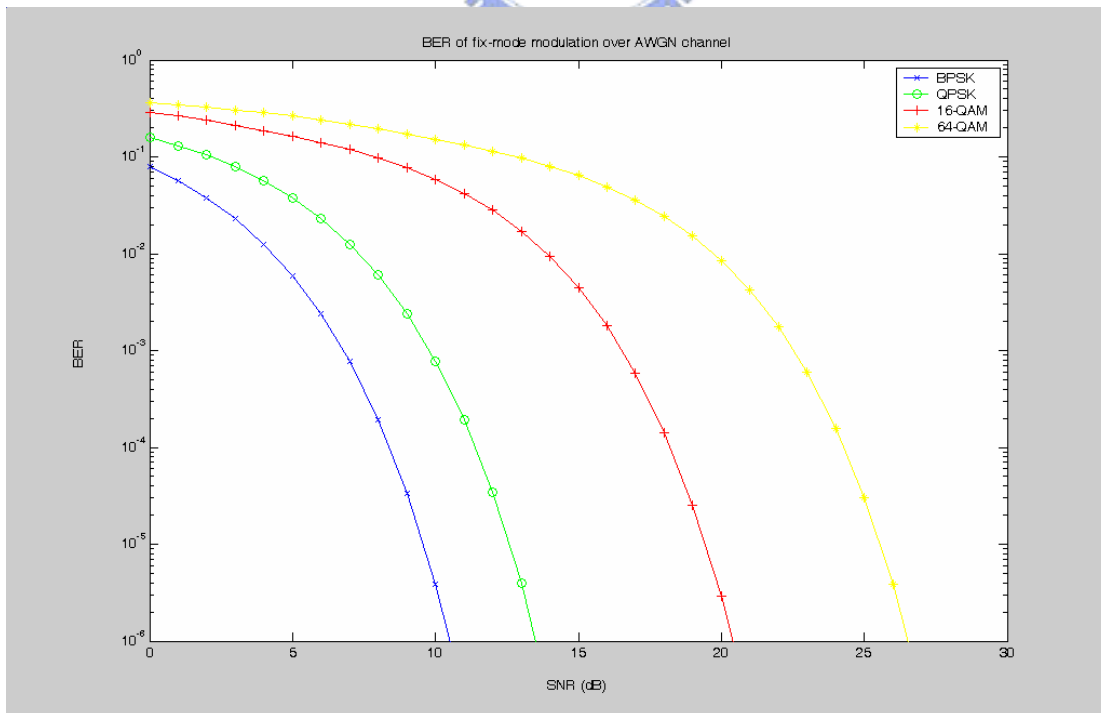

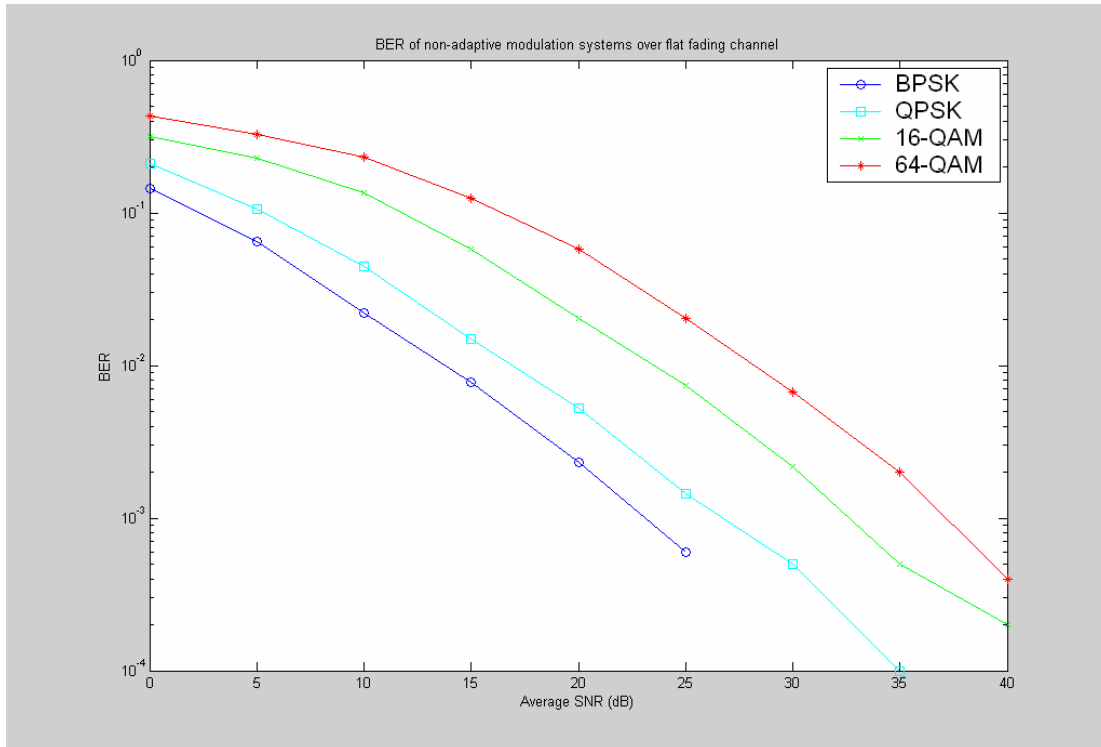Figure 1.1: BER of fix-mode modulation schemes over AWGN channel

2

Figure 1.2: BER of fix-mode modulation schemes over Rayleigh fading channel

1.2 Adaptive modulation

In a fading channel environment, the transmission parameters such as modulation mode, code rate, and transmission symbol rate can be adjusted to fit for current channel condition. The above techniques are called adaptive modulation. There are many indicators such as BER (bit error rate), RSSI (received signal strength indicator), SNR (signal to noise ration) and their associated statistics capable of being used to evaluate the fading channel condition. In this thesis, adaptation of modulation mode is concerned and instantaneous signal to noise ratio (iSNR) is used as a metric to select a suitable modulation mode. The transmitted signal power and noise power are assumed constant and known. Thus before transmitting a burst, the

3

transmitter selects a suitable modulation mode according to the predicted iSNR of the received signal, as in Fig. 1.3. The adaptation is on a burst-by-burst (BbB) basis, and the channel is assumed invariant during a burst period (quasi-static).
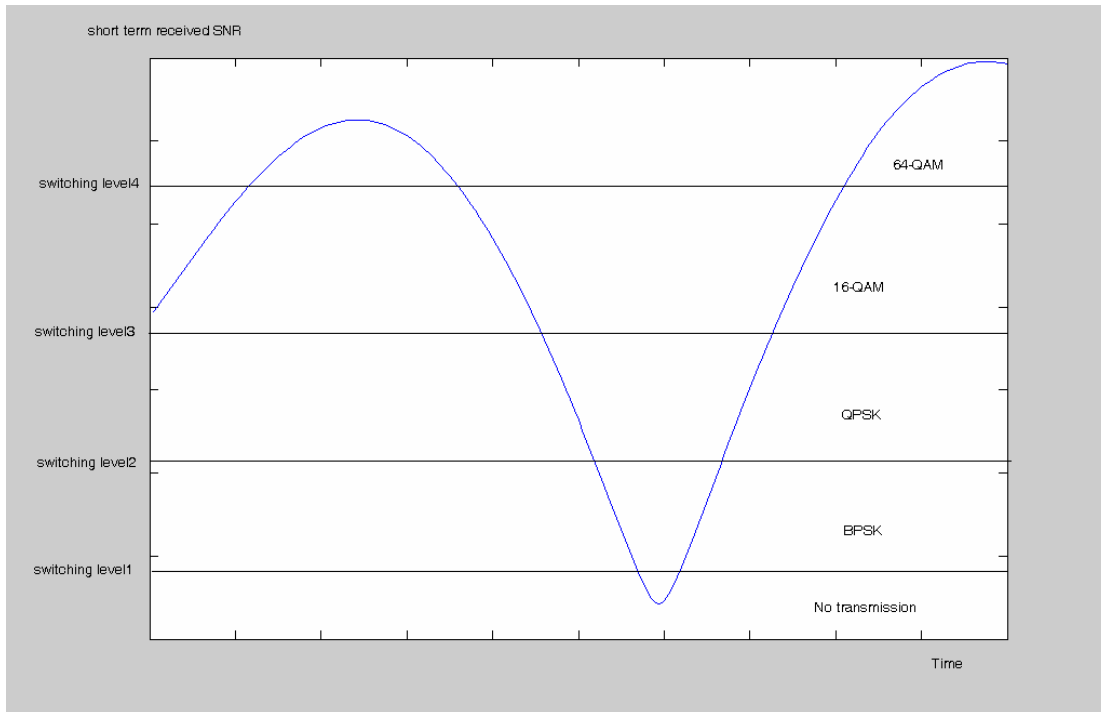

Figure 1.3: Choosing the modulation mode according to iSNR

The receiver must know the modulation mode parameters for the current receiving burst in some way. This information can either be conveyed within the transmission symbol itself, with loss of effective data throughput, or the receiver can try to estimate the parameters by means of blind detection. In practical systems, the former is often adopted.

1.3 Mode parameter signaling

Both TDD (time division duplex) and FDD (frequency division duplex)

schemes can be used for adaptive modulation systems. In a TDD/TDMA system, the uplink and downlink time slots are separated into two halves of a TDMA frame, as shown in Fig. 1.4. In TDD scheme, the uplink and downlink channels use the same transmission frequencies and are called reciprocal. In the uplink transmission, the channel quality is estimated at the base station (BS) and subsequently an appropriate transmission mode is selected for its next downlink transmission. This is achieved by exploiting the reciprocity between the uplink and downlink channels. Having selected the modulation mode, a delay of half a TDMA frame is incurred at the BS before the downlink transmission is activated. This regime is called open-loop controlled adaptive modulation.
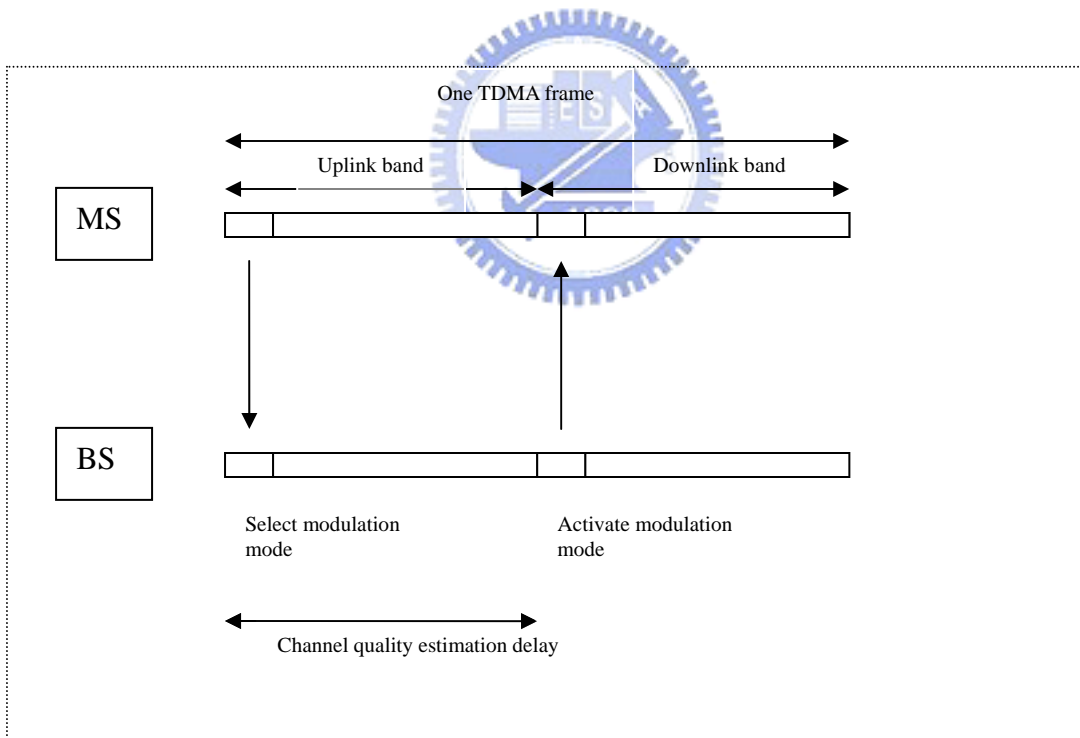

Figure 1.4: Sub-frame based TDD/TDMA system

Next consider the FDD/TDMA scheme in Fig. 1.5. In FDD system, the uplink and downlink use different bank and the channel reciprocity in TDD is not appropriate more. Thus the signaling of the mode parameters is on a

close-loop basis. In the uplink transmission, the channel quality is estimated at the BS, in order to select the next uplink transmission mode. The selected uplink mode is then conveyed to the mobile station (MS) with the aid of control symbols during the next downlink transmission and utilized by the MS in the next uplink transmission. Because of the close-loop signaling regime, the delay incurred by the system is equal to the duration of a TDMA frame. Since the maximum delay that can be tolerated by an adaptive modulation systems is the same regardless of the type of the system (TDD or FDD), the open-loop system is better for adaptive modulation because of its lower delay. In the simulation in chapter 4, the channel quality estimation delay is assumed to be one transmission burst, the same as in TDD case.
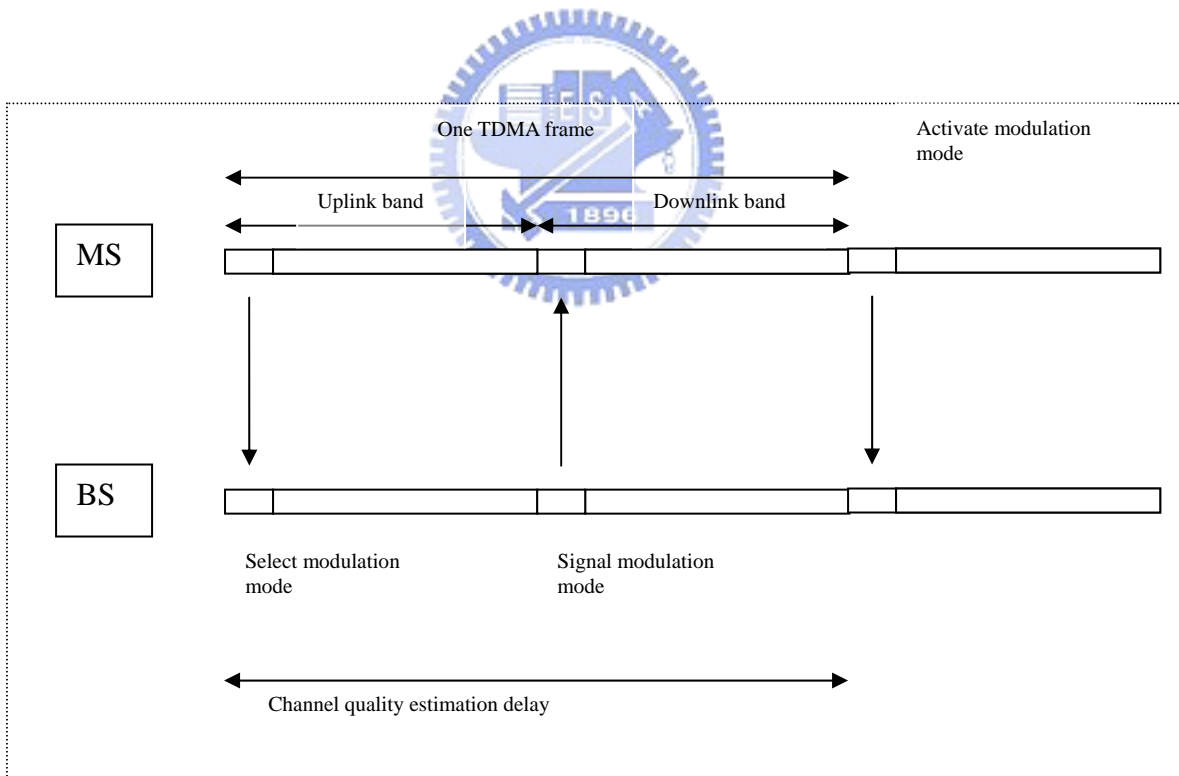

Figure 1.5: Sub-frame based FDD/TDMA system

Chapter 2

Switching level optimization for adaptive modulation

_____

In an adaptive modulation system, one critical problem is the determination of the switching levels between the modulation modes. In this chapter, several methods in the literature are discussed. Among them, based on Torrance's method [2] and Lagrange method [3] we propose a fast algorithm to determine the switching levels. The proposed method is a simplification of Torrance's method and its lower complexity make it more practical than the original method in the wireless channel.

2.1 System description

For a K-mode adaptive modulation scheme, there are K-1 switching levels to be determined. The mode is selected according to some channel state measure ξ by the rule:

$$\text{choose mode } k, \text{ when } s_k \leq \xi < s_{k+1} \tag{2.1}$$

In this chapter we consider a five-mode adaptive modulation system including no transmission, BPSK, QPSK, 16QAM, and 64QAM. Some symbols used later are listed in table 2.1. For simplicity, only narrow band

signal in flat fading channel is considered. The instantaneous SNR (iSNR), γ, is used as the channel state measure and perfect channel estimation is assumed. Frequency-nonselective Rayleigh fading channel is considered, so that the probability density function (pdf) of γ is given as [4]:
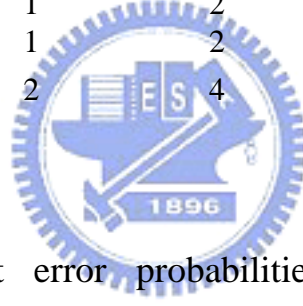
$$f_{\bar{\gamma}}(\gamma) = \frac{1}{\bar{\gamma}} e^{\frac{\gamma}{\bar{\gamma}}}, \gamma \geq 0 \tag{2.2}$$

where $\bar{\gamma}$ is the average SNR.

Table 2.1: parameters of the 5-mode adaptive modulation scheme,

where b_k: bits/symbol for mode k . m_k: constellation size of mode k

mode	No Tx	BPSK	QPSK	16QAM	64QAM
k	0	1	2	3	4
b_k	0	1	2	4	6
m_k	0	2	4	16	64

The instantaneous bit error probabilities (iBEP), $p_m(\gamma)$, of the modulation modes are function of the iSNR. For the Gray-mapped square QAM and with coherent detection and perfect timing synchronization, they are given as [5]:

$$p_{BPSK}(\gamma) = Q(\sqrt{2\gamma})$$

$$p_{QPSK}(\gamma) = Q(\sqrt{\gamma})$$

$$p_{16QAM}(\gamma) = 0.75Q(\sqrt{\frac{\gamma}{5}}) + 0.5Q(3\sqrt{\frac{\gamma}{5}}) - 0.25Q(5\sqrt{\frac{\gamma}{5}}) \tag{2.3}$$

$$p_{64QAM}(\gamma) = \frac{7}{12}Q(\sqrt{\frac{\gamma}{21}}) + \frac{1}{2}Q(3\sqrt{\frac{\gamma}{21}}) - \frac{1}{12}Q(5\sqrt{\frac{\gamma}{21}})$$

$$+ \frac{1}{12}Q(9\sqrt{\frac{\gamma}{21}}) - \frac{1}{12}Q(13\sqrt{\frac{\gamma}{21}})$$

where $Q(x) = \dfrac{1}{\sqrt{2\pi}} \displaystyle\int_x^\infty e^{-\frac{y^2}{2}} dy$.

To evaluate an adaptive modulation system, two important performance indicators are often used. They are the average bit error rate (BER) and the average throughput (in bits/symbol; BPS) of the adaptive modulation scheme. The average BPS is defined as:

$$B_{avg}(\bar{r};s) = \sum_{k=0}^{K-1} b_k \int_{s_k}^{s_{k+1}} f_{\bar{\gamma}}(r)\,dr \tag{2.4}$$

By the definition, BPS stands for the average transmission bit per symbol for the adaptive modulation scheme.

The average BER is defined as:

$$P_{avg}(\bar{\gamma};s) = \frac{1}{B_{avg}(\bar{\gamma};s)} \sum_{k=0}^{K-1} b_k P_k \quad , \tag{2.5}$$

where P_k is the mode-specific average BER defined as $P_k = \displaystyle\int_{s_k}^{s_{k+1}} p_{m_k}(r) f_{\bar{\gamma}}(r)\,dr$

2.2 Limiting the maximum allowable iBEP

From (3), the BER curves for the five modulation modes are plotted in Fig. 2.1. The first and simplest method to find the optimum levels is by using the curves. The method was proposed by Webb and Steele [6]. Normally, it's desired that average BER of the system is lower than some threshold, P_{th}. To meet this requirement, Webb and Steele using the intuitive concept that if all modulation modes are used only when satisfying the constraint, that is, in the situation that $p_m(\gamma) \le P_{th}$, then the overall BER constraint is satisfied. The set of switching levels **S** (in dB) is given by

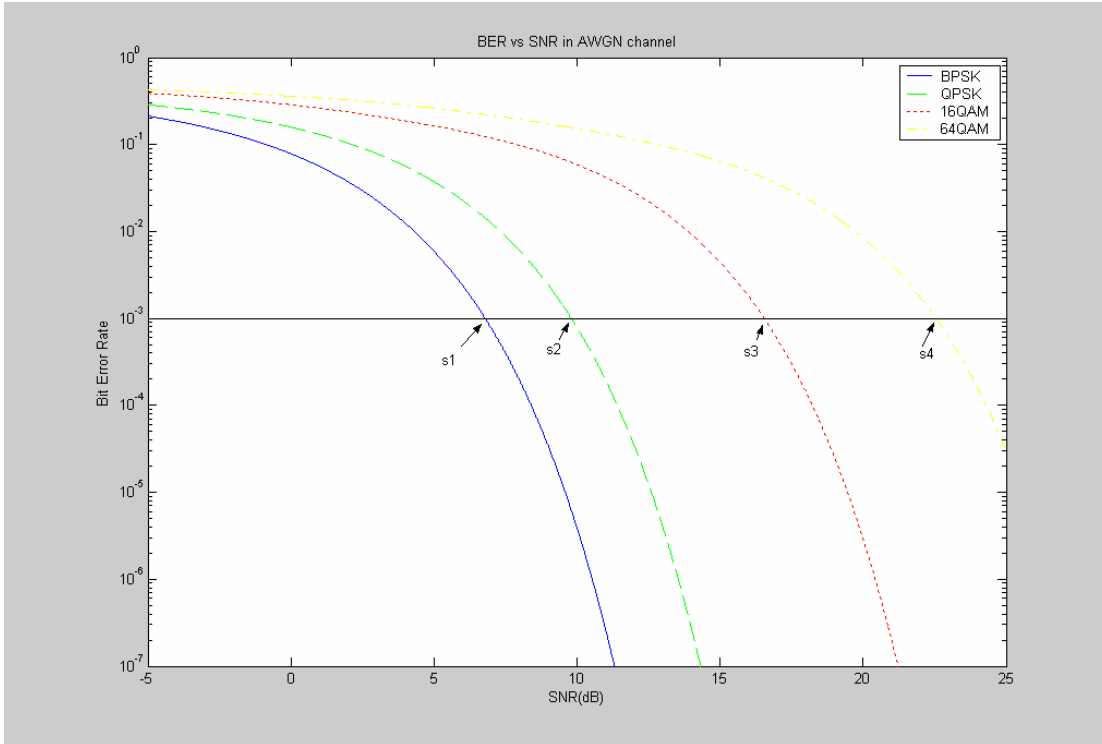$$S = \{s_0 = -\infty, s_k \mid p_{m_k}(s_k) = P_{th}, \forall k \ge 1\} \tag{2.6}$$

Figure 2.1: BER of various M-QAM schemes over AWGN channel

For our five mode adaptive modulation system, the switching levels gotten by this method at the target $BER=10^{-2}, 10^{-3}$ and 10^{-4} are shown in table 2.2.

Table 2.2: SNR thresholds (in dB) for various modulation modes

Target BER	No TX	BPSK	QPSK	16QAM	64QAM
10^{-2}	$-\infty$	4.32	7.33	13.9	19.73
10^{-3}	$-\infty$	6.78	9.79	16.54	22.54
10^{-4}	$-\infty$	8.39	11.4	18.22	24.3

The above method is conservative because the BER requirement is achieved at any time and the resulting average SNR may be low far from the target BER needed. Thus we can further lower the switching levels to increase throughput while still satisfying the average BER constraint.

Besides, it's desired that the system can adjust the levels to different channel conditions which in our case are the average SNR of the received signal. Several advanced methods are discussed in the following sections.

2.3 Torrance's method

Usually the optimization of the switching levels is to achieve the goal maximizing the throughput (average transmitted bit/symbol) under the constraint that average BER equal to some pre-determined target. In the last section, the method to find the switching levels by limiting the peak instantaneous BEP is discussed. Although being simple, the method is too conservative and it's beneficial to lower the levels to increase the throughput.

Once the levels $\mathbf{S}$ are determined, the average BER $P_{avg}(\bar{\gamma};\mathbf{S})$ and average throughput $B_{avg}(\bar{\gamma};\mathbf{S})$ are also determined. To consider the two performance measures simultaneously, Torrance proposed the following cost function:

$$\Omega(\mathbf{S};\bar{\gamma}) = 10\log_{10}(\max\{P_{avg}(\bar{\gamma};\mathbf{S})/P_{th},1\}) + B_{\max} - B_{avg}(\bar{\gamma};\mathbf{S}) \qquad (2.7)$$

where cost of BER: $10\log_{10}(\max\{P_{avg}(\bar{\gamma};\mathbf{S})/P_{th},1\})$

cost of throughput: $B_{\max} - B_{avg}(\bar{\gamma};\mathbf{S})$

P_{th} : the target average BER

$B_{\max}$: Bit-per-symbol (BPS) throughput of the modulation of the highest order.

The cost function is composed of two parts: cost of BER and cost of throughput. The switching levels are selected as the solution to minimize the

cost function. As the switching levels become larger, $P_{avg}(\bar{\gamma};S)$ and $B_{avg}(\bar{\gamma};S)$ both become larger. So the cost of BER becomes larger and the cost of throughput becomes smaller. On the other hand, when the switching levels become smaller, the cost of BER becomes smaller and the cost of throughput becomes larger. When P_{avg} is smaller than the target BER, the cost of BER doesn't change corresponding to the variation of switching levels, and the average BER is maintained at about the target BER through this way.

For a K-mode adaptive modulation system, there are K-1 levels to be determined. Thus the problem is a multi-variable minimization problem. The solution can be found by applying the multi-dimensional optimization technique called Powell's minimization and an example in which target BER is setting at 10^{-3} is shown in Fig. 2.2.
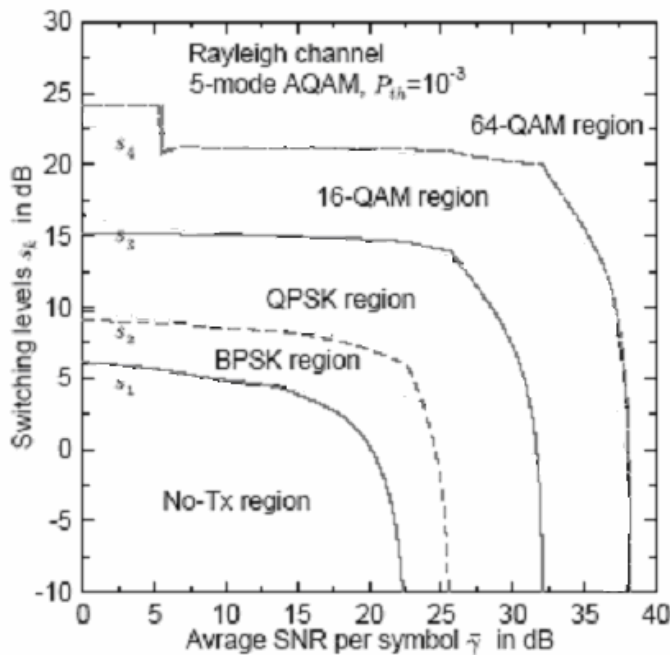

Figure 2.2: Switching levels found by Torrance's method for each average
SNR (from [2])

2.4 Lagrange optimization method

In the last section, the method using Torrance's cost function to determine the switching levels for each average SNR value is discussed. In this section, another method using the Lagrangian multiplier technique to determine the levels will be considered.

As mentioned in the last section, the goal of the optimization is to maximize the average throughput under the constraint that average BER equal to some threshold. So it's a constrained maximization problem, and can be solved using the Lagrange multiplier.

The problem is as following:

$$\max_{s} \quad B_{avg}(\bar{\gamma}; s)$$
$$\text{subject to } P_{avg}(\bar{\gamma}; s) = P_{th} \tag{2.8}$$

In (2.8), the constraint equation can be displaced by $P_R(\bar{\gamma}; s) = P_{th} B_{avg}(\bar{\gamma}; s)$, where $P_R(\bar{\gamma}; s) \triangleq \sum_{0}^{K-1} b_k P_k$ for the simplicity of the following calculation.

In the standard practice, the modified objective function is formulated as:

$$\Lambda(\bar{\gamma}; s) = B_{avg}(\bar{\gamma}; s) + \lambda \left\{ P_R(\bar{\gamma}; s) - P_{th} B_{avg}(\bar{\gamma}; s) \right\}$$
$$= (1 - \lambda P_{th}) B_{avg}(\bar{\gamma}; s) + \lambda P_R(\bar{\gamma}; s) \tag{2.9}$$

Through the introducing of the Lagrange multiplier λ, the constrained maximization problem is transformed to an unconstrained one as:

$$\frac{\partial \Lambda(\bar{\gamma}; s)}{\partial s} = 0 \text{ and } P_R(\bar{r}; s) = P_{th} B_{avg}(\bar{r}; s) \tag{2.10}$$

Taking our five-mode scheme as example, in addition to the unknown λ, there are four variables to be determined. So there are totally five unknowns have to be solved (of course only four of them is needed to us) from the five equations in (2.10). Thus in the usual condition, there are one set of

particular solution to the problem. The above condition can't be true when $P_R(\bar{r};s)=P_{th}\bar{B}_{avg}(\bar{r};s)$ can't be satisfied, that is, when $\bar{\gamma}$ is so large that $P_R(\bar{r};s)<P_{th}\bar{B}_{avg}(\bar{r};s)$ for all possible s values.

Although we know that usually the problem has a particular solution, it's still hard to get the levels because in our case the five equations each still contain more than two variables. Among them, four equations contain λ and one switching level and the other contain all the four levels. One calculation procedure is derived in [2], in which λ is   eliminated after some operations and the switching levels can be derived easier.

Define the Lagrange-free function as:

$$y_k(s_k)=\frac{1}{b_k-b_{k-1}}\{b_k p_{m_k}(s_k)-b_{k-1}p_{m_{k-1}}(s_k)\} \ , \ k=2,3,...K-1 \tag{2.11}$$

Then the switching levels can be related by:

$$y_k(s_k)=y_1(s_1) \ , \ k=2,3,...K-1 \tag{2.12}$$

So if s_1 (or any s_k) is known as $a_1(a_k)$, other switching levels $s_i=a_i$ can also be calculated as in Fig 2.3 in which the Lagrange-free functions are shown.
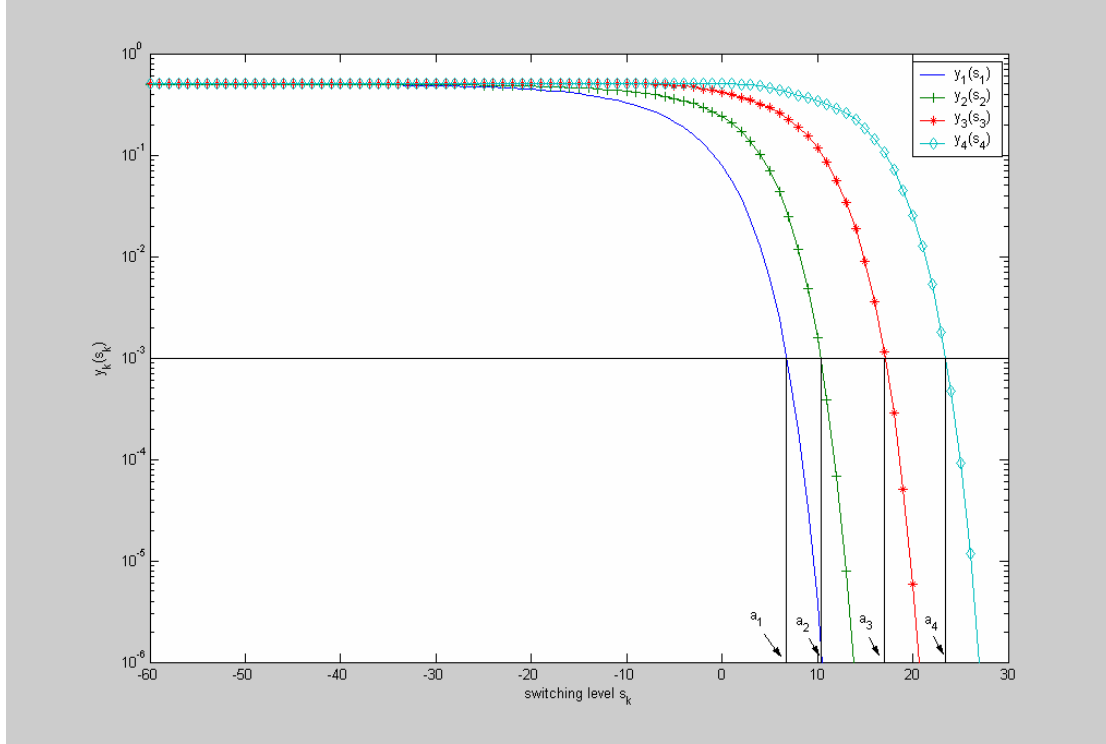
Figure 2.3: Lagrange-free functions in the Lagrange method

Now the only problem is how we know the value of s_1. It can be done by using the constraint equation. Define the constraint function $Y(\bar{r}, s(s_1))$ as:

$$Y(\bar{r}, s(s_1)) \triangleq P_R(\bar{r}, s(s_1)) - P_{th}B_{avg}(\bar{r}, s(s_1)) \tag{2.13}$$

Then for each average SNR $\bar{\gamma}$, the value of s_1 making the constraint function be zero is what we want. In fig 2.4, the constraint functions for different target BER at $\bar{\gamma} = 30dB$ and in fig 2.5, for different average SNR at $P_{th} = 10^{-3}$ are shown.
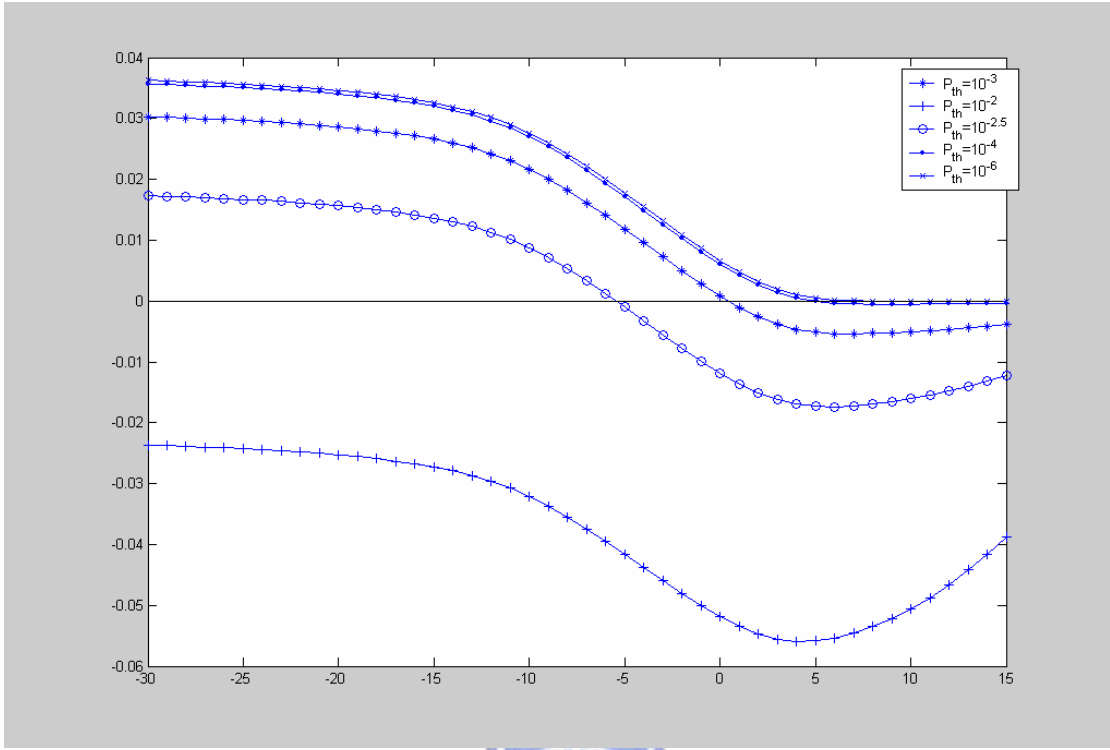
Fig 2.4: Constraint functions for different target BER when average SNR
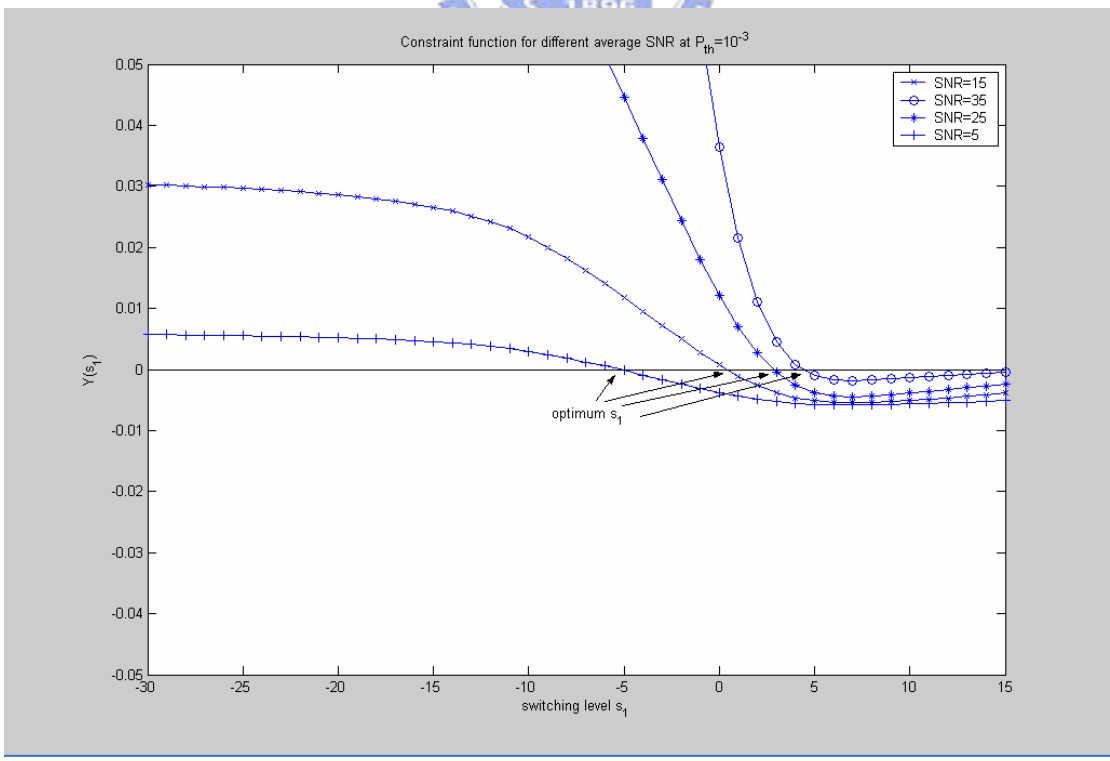
$$\overline{\gamma} = 30dB$$

Fig 2.5: Constraint functions for different average SNR at $P_{th} = 10^{-3}$

After knowing the optimum value of s_1, the other optimum switching levels can be derived through (2.12). The switching levels derived by Lagrange method at $P_{th} = 10^{-2}$ and 10^{-3} for average SNR from 0dB to 40dB are shown in fig 2.6.
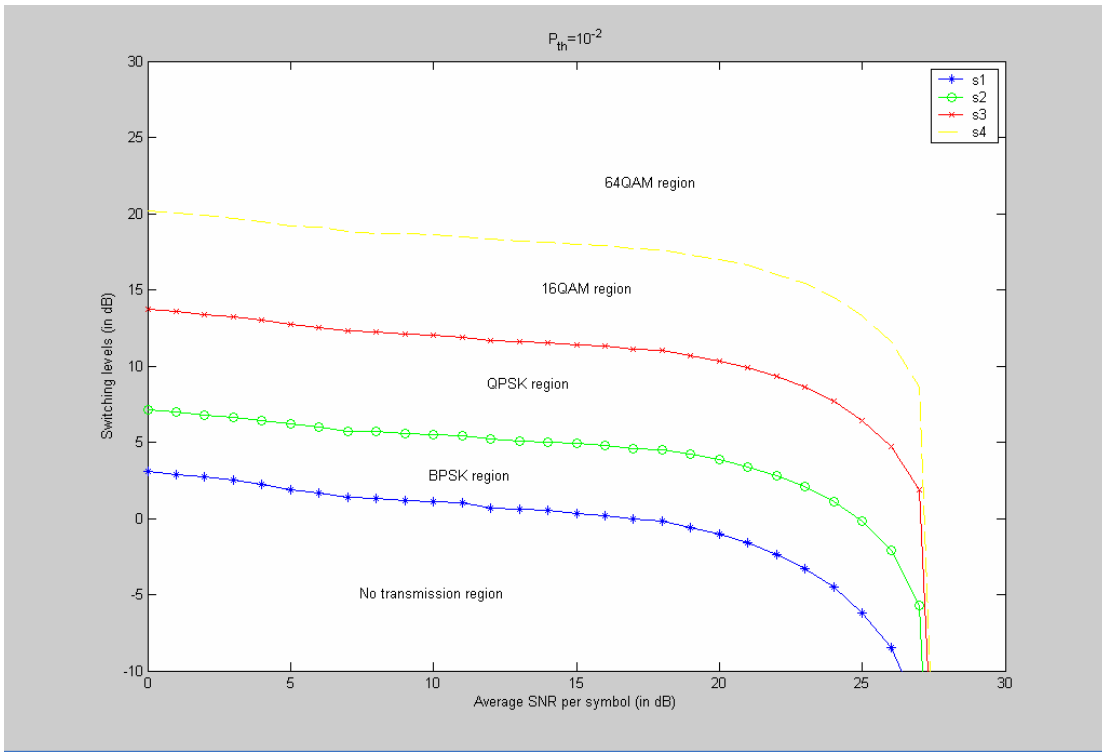

Fig 2.6(a): Switching levels derived by Lagrange method at $P_{th} = 10^{-2}$
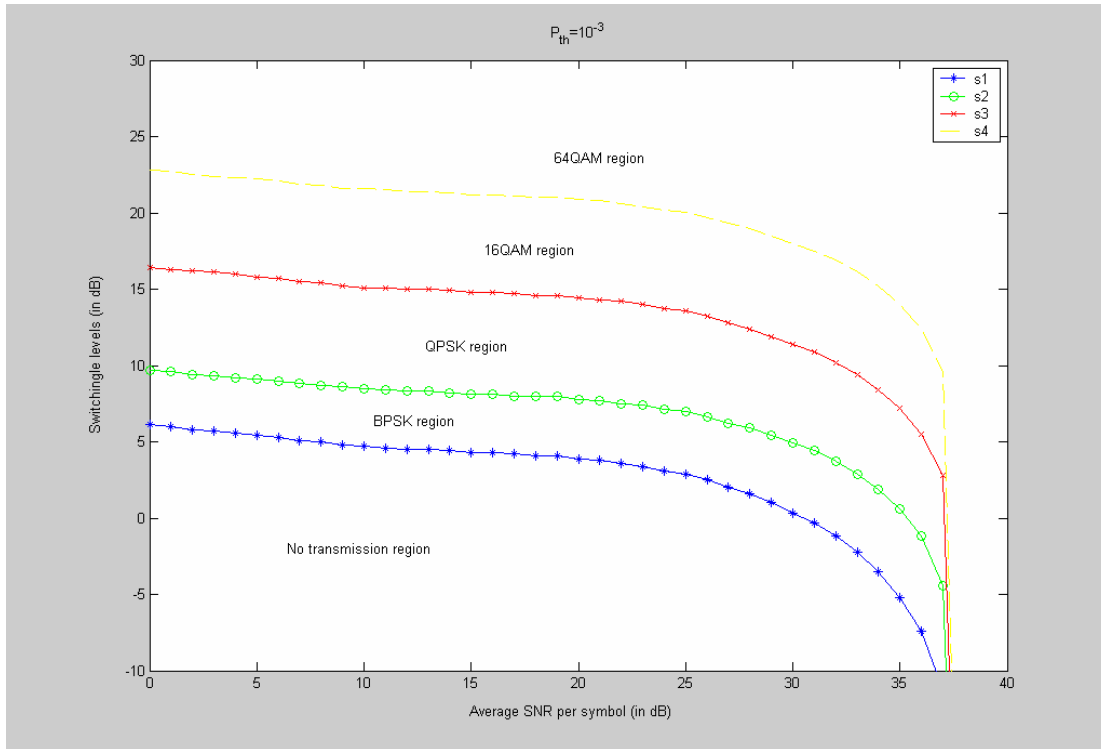
Fig 2.6(b): Switching levels derived by Lagrange method at $P_{th} = 10^{-3}$

2.5 Two-mode Torrance's method and a further simplified method

One of the disadvantages of the Torrance's method is the high complexity due to solving the optimization problem of multi-variables. If we can determine the switching levels sequentially in some way, the complexity will be reduced. To do this, two methods are proposed. The first method is a special case of the Torrance's method, and the other is a further simplified version.

Consider an adaptive modulation scheme which only contains two modulation modes, for example, BPSK and QPSK. Employing Torrance's method for the scheme, the switching level between the two modes can be found and used as the corresponding level for the original five-mode case.

The other three levels can be derived in the same way. The two-mode Torrance cost functions for several cases are shown in fig 2.7.
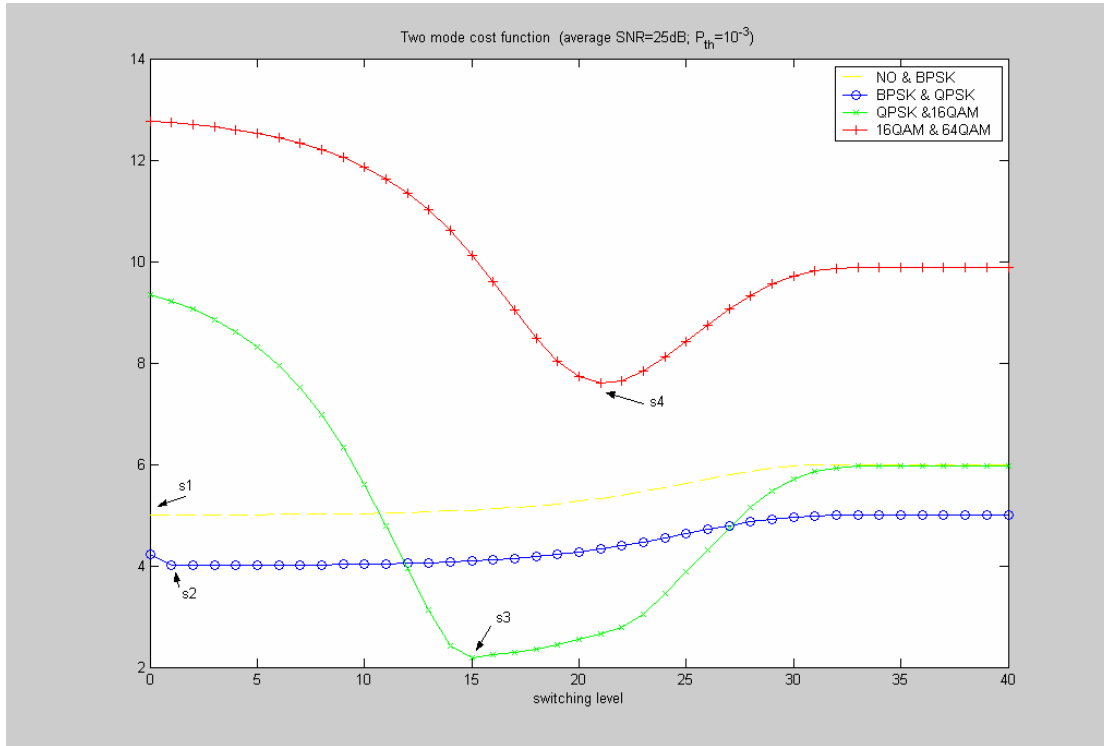

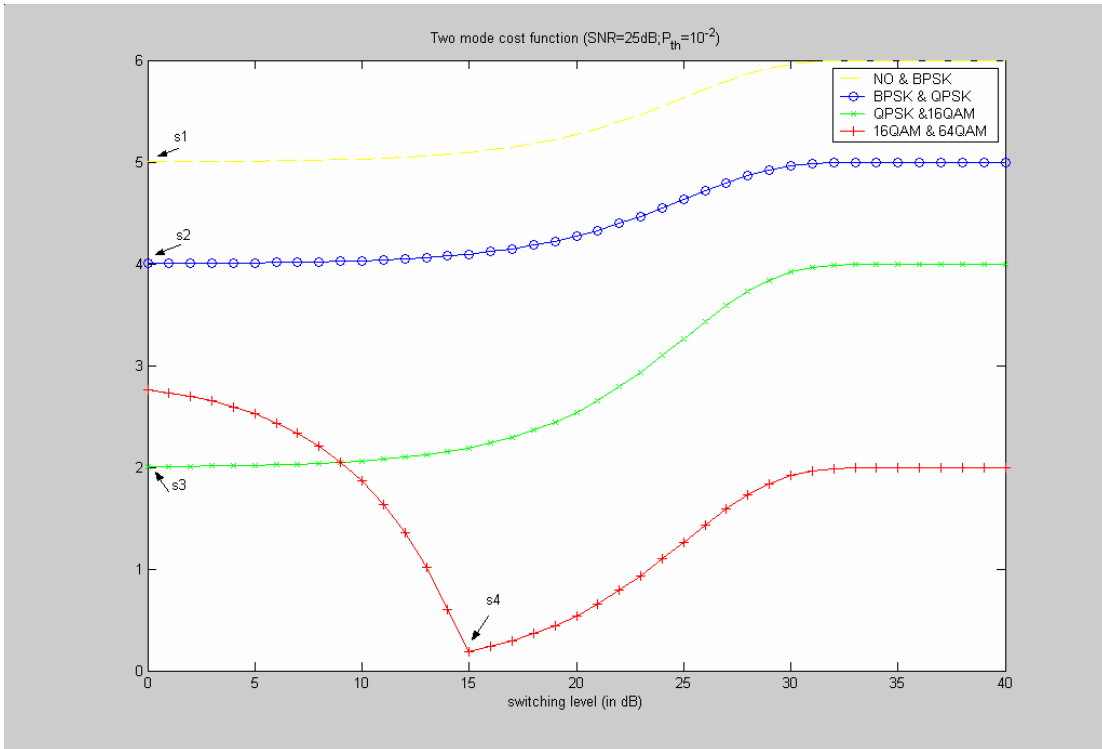Fig 2.7(a): Two mode Torrance cost function.   Average SNR=25dB; $P_{th} = 10^{-3}$

Fig 2.7(b): Two mode Torrance cost function. Average SNR=25dB; $P_{th} = 10^{-2}$
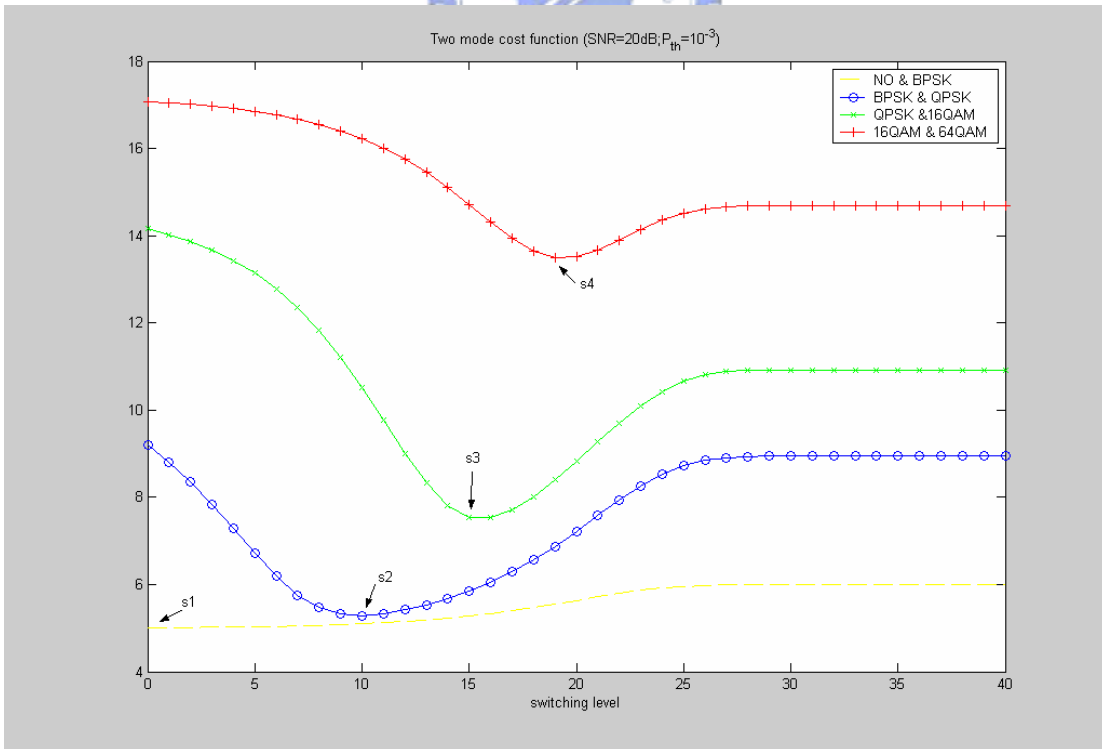

Fig 2.7(c): Two mode Torrance cost function. Average SNR=20dB; $P_{th} = 10^{-3}$

The two-mode cost function method can be further simplified. In the following, we try to define a partial cost function for each single mode from the original two-mode Torrance cost function through some approximation. Then the modulation mode can be selected easily as that has the smallest cost.

To design the single-mode partial cost function to fit our requirement, some approximation must be made. The first step is to neglect the target BER threshold and logarithm operation in the cost function temporarily. Then replace the average BER cost part by the sum of mode specific error probabilities (the only difference is the dividing of average BPS B_{avg}). The last action can be done because in the single-mode case, "average BPS" is meaningless and can be included into the final constant in the formulation.

After the approximations, taking BPSK and QPSK for example, the two-mode Torrance cost function is modified as:

$$(\int_0^{s_1} P_B(r)f(r,\bar{r})dr + \int_{s_1}^{\infty} P_Q(r)f(r,\bar{r})dr) + (B_{max} - \int_0^{s_1} 1 f(r,\bar{r})dr - \int_{s_1}^{\infty} 2 f(r,\bar{r})dr)$$

$$= (\int_0^{s_1} P_B(r)f(r,\bar{r})dr + P_Q(\bar{r}) - \int_0^{s_1} P_Q(r)f(r,\bar{r})dr) + (B_{max} - \int_0^{s_1} 1 f(r,\bar{r})dr - 2 + \int_0^{s_1} 2 f(r,\bar{r})dr) \qquad (2.14)$$

$$= (\int_0^{s_1} P_B(r)f(r,\bar{r})dr - \int_0^{s_1} 1 f(r,\bar{r})dr) - (\int_0^{s_1} P_Q(r)f(r,\bar{r})dr - \int_0^{s_1} 2 f(r,\bar{r})dr) + C$$

In (2.14), $P_Q(\bar{r}) = \int_0^{\infty} P_Q(r)f(r,\bar{r})dr$, and $C = P_Q(\bar{r}) + B_{max} - 2$ both are constants independent of the switching level. Thus what important to decide the level can be related to the following partial cost function:

$$C_i'(x;\bar{r}) \triangleq \int_0^x P_i(r)f(r,\bar{r})dr - i\int_0^x f(r,\bar{r})dr \qquad (2.15)$$

To make the partial cost function to be a monotonically decreasing function of the SNR, the above function is normalized to the integration interval as:

$$C_i\,''(x;\bar{r}) \triangleq \frac{\left(\int_0^x P_i(r)f(r,\bar{r})dr - i\int_0^x f(r,\bar{r})dr\right)}{\int_0^x f(r,\bar{r})dr} = \int_0^x P_i(r)\frac{f(r,\bar{r})}{\int_0^x f(r,\bar{r})dr}dr - i \qquad (2.16)$$

It can be seen that the partial cost function is sum of two terms as in the original Torrance cost function (2.7). The first term in (2.16) is cost of BER, and the second term is cost of throughput. As in (2.7), each part of the cost function should be properly weighted. Finally, the partial cost function for each single mode is defined as:

$$C_i(x;\bar{r}) = 10\log_{10}\max\left(\frac{\int_0^x P_i(r)\dfrac{f(r,\bar{r})}{\rho\int_0^x f(r,\bar{r})dr}dr}{P_{th}},1\right) - i \qquad (2.17)$$

where ρ is a normalization constant and can be adjusted according to our needs such as increasing throughput or decreasing BER.

In the single-mode cost function method, the modulation mode is selected as one who has the smallest cost. In fig 2.8, the partial cost functions for the five-mode scheme at average SNR=25dB, $P_{th} = 10^{-3}$, and $\rho = 45$ are shown as an example.
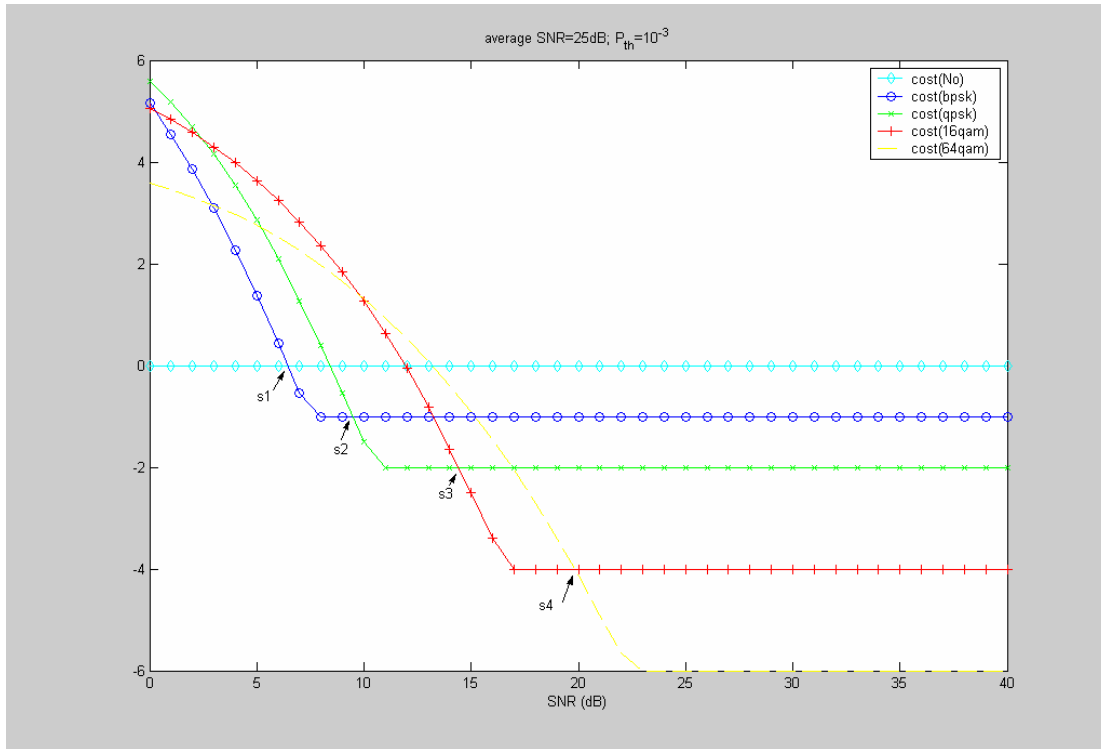
Fig 2.8: Partial cost functions. Average SNR=25dB; $P_{th} = 10^{-3}; \rho = 45$

We can adjust the switching levels for our needs by changing the predetermined parameter ρ. When ρ is increasing, the proportion of BER cost in the overall cost decreases, and this means the BER cost measure becomes less and BPS cost measure becomes more important. Thus the switching levels will become smaller. On the contrary, when ρ is decreasing, the switching levels will become larger. Some examples are shown in table 2.3.

Table 2.3: Switching levels for different ρ. Average SNR=25dB; $P_{th} = 10^{-3}$

	s1	s2	s3	s4
$\rho = 20$	10	13	18	25
$\rho = 40$	7	10	15	20.5
$\rho = 60$	5	8	13	18

Usually the cost function stops decreasing with increasing average SNR when the partial BER equals to the target BER. That is when equation 2.18 holds.

$$\int_0^x P_i(r) \frac{f(r,\bar{r})}{\rho \int_0^x f(r,\bar{r})dr} dr = P_{th} \qquad (2.18)$$

When average SNR is small, the partial BER may saturate before reaching the target BER. Figure 2.9 (a) and(b) show the partial BER functions and partial cost functions at average SNR=18dB. It can be seen that partial BER of 64-QAM saturates at about 23dB before reaching the target BER. Thus the corresponding partial cost function can't reach its final value -6 as in larger average SNR case and there will be no intersection between partial BER functions of 16-QAM and 64-QAM. As the average SNR decreases, similar event will occur for 16-QAM, QPSK, and BPSK sequentially. In these situations the one –mode method can't work well and the switching levels will be selected as some pre-determined values.
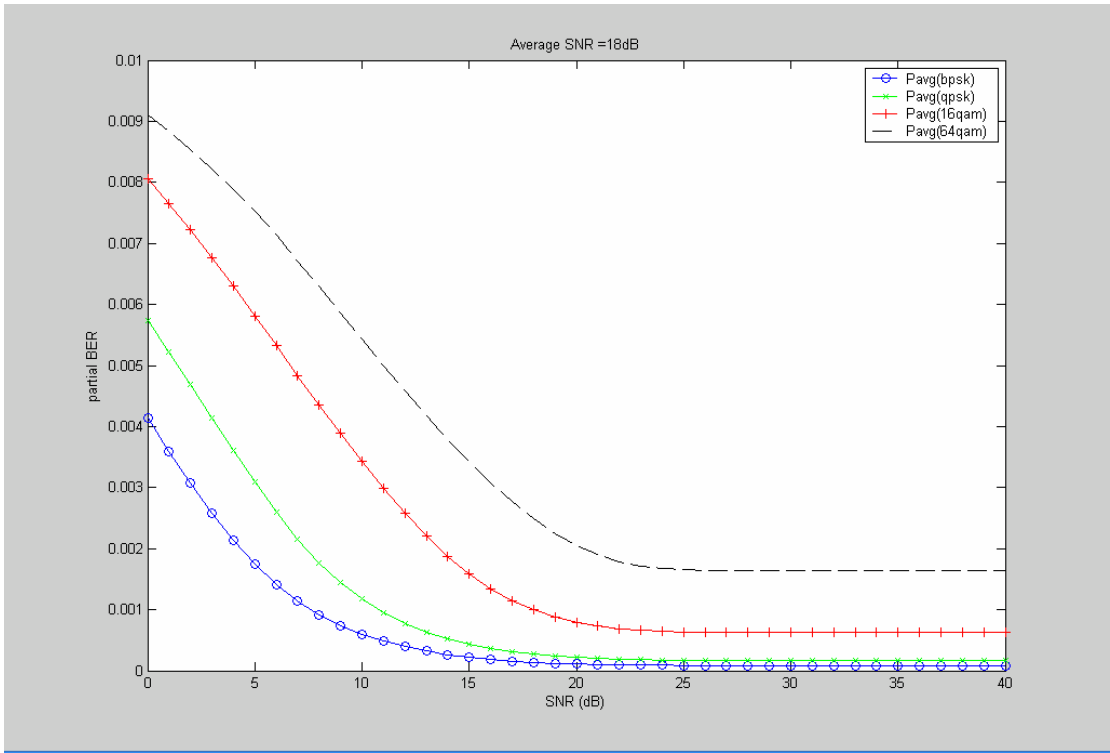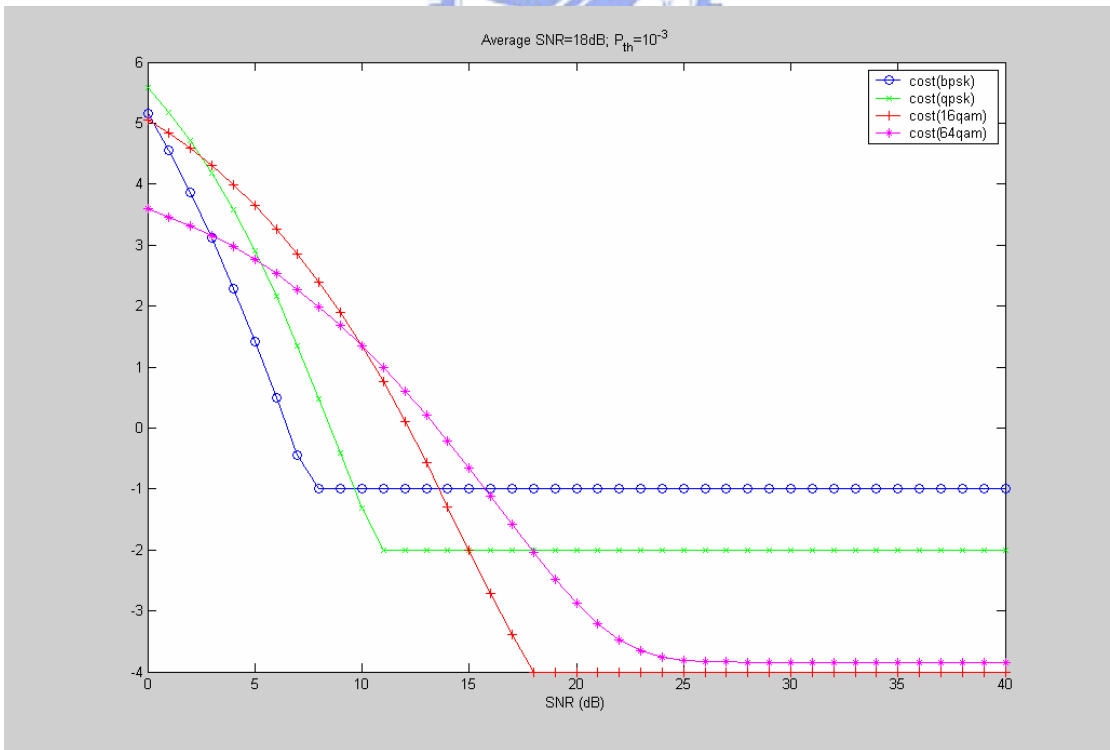
Fig 2.9(a): BER functions at average SNR=18dB

Fig 2.9(b): cost functions at average SNR=18dB

25

As Torrance's method and Lagrange method, the one-mode method also determines switching levels under different channel fading condition. Figure 2.10 shows the determined levels when target BER is 10^{-3} and ρ is set to 45.
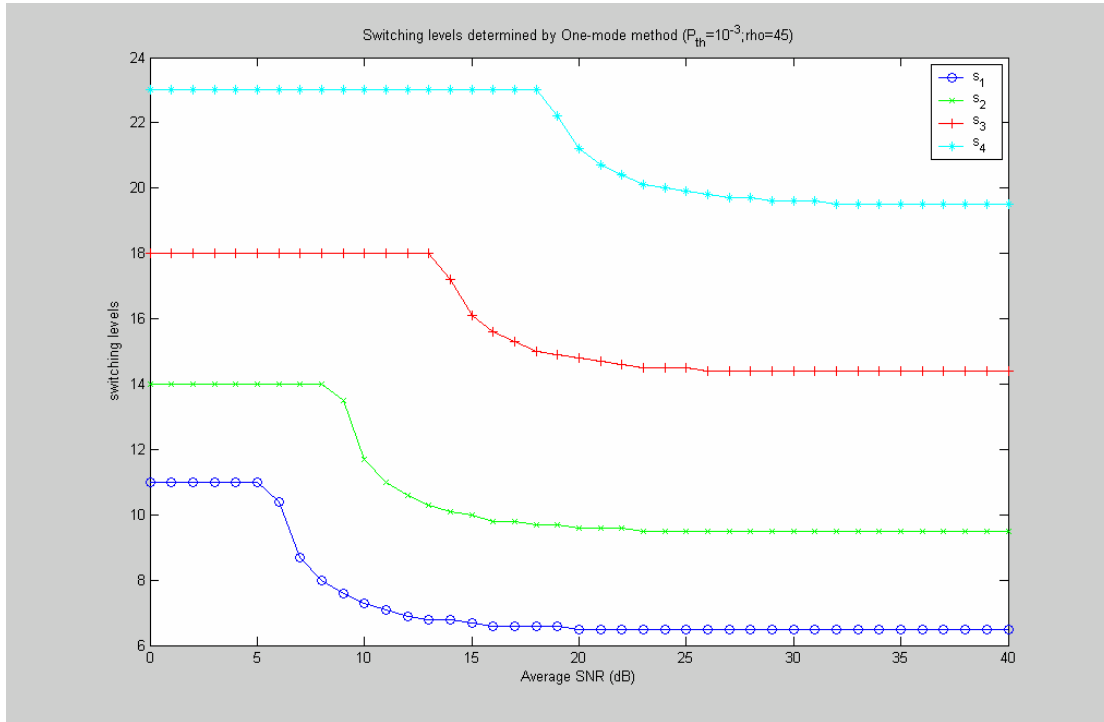

Figure 2.10: Switching levels derived by one-mode method at $P_{th} = 10^{-3}$

From section 2.4, we know that in the Lagrange method, once one of the switching levels is known, the others can be derived from (2.12). Thus the proposed method provides a simple way to get the first switching level, without solving the complex equation (2.13). After some experiment, the values of ρ making s_1 the same as those in Lagrange method are shown in table 2.4.

Table 2.4: ρ value to make s1 the same as in Lagrange method

Average SNR(dB)	15	20	25
s1(dB)	4.3	3.9	2.9
ρ	77	92	110

2.6 Simulation result and conclusion

Several methods to determine the switching levels for adaptive modulation are discussed in the above sections. Among them, limiting the iBEP is the simplest but too conservative and can't adjust to the varying channel statistic which in our case is average SNR. Lagrange method provides the exact solution to the problem (2.8), maximizing the throughput under the constraint that average BER equal to some target. Although optimum, Lagrange method is complex especially when deriving s_1 which is done by setting equation (2.13) to be zero.

The method using Torrance's cost function provides an indirect way to solve the problem by transforming it to the minimization of the cost function. It is obvious that the BER constraint can't be satisfied perfectly. Besides, the problem is still complex because although unconstrained, it's still a multi-variable optimization problem.

Two-mode Torrance method is a modified version of the original one. It considers only two modes once and thus converts the multi-variable optimization problem to several one-variable optimization problems.

The proposed method tries to derive a suitable cost function for each mode, and the mode selection can be done based on the comparison of the costs. The cost function defined in (2.17) satisfies the needs. Performance of the method depends on the normalization factor ρ which can be

pre-determined and adjusted for practical requirement. By setting ρ to some particular value, the proposed method can be used as an alternate to derive the first switching level in the Lagrange method, avoiding the most complex part.

The determined switching levels and resultant performances at $P_{th} = 10^{-3}$, for average SNR=15, 20, and 25 dB from the five methods are shown in table 2.5. It can be seen that the average BER performance in Lagrange method is about the target BER (theoretically, it will fixed at the target if the values of the levels are more precise), while in other methods it is not the case. So if the BER constraint is to be obeyed exactly, the Lagrange solution is recommended and the one mode method can be used to derive s_1.

Table 2.5(a): switching levels (in dB) and resultant performances from the five methods. Average SNR=25dB; $P_{th} = 10^{-3}$

	s1	s2	s3	s4	P_{avg}	B_{avg}
Limiting iBEP	6.8	9.8	16.5	22.5	1.0E-04	4.823
Torrance	$-\infty$	3	14	20.4	1.0E-03	5.255
Two mode	$-\infty$	1	15	21	8.1E-04	5.149
Lagrange	2.9	7	13.6	20	1E-03	5.296
One mode ($\rho = 45$)	6	9	14	20	9.3E-04	5.268

Table 2.5(b): switching levels (in dB) and resultant performances from the

five methods. Average SNR=20dB; $P_{th} = 10^{-3}$

	s1	s2	s3	s4	P_{avg}	B_{avg}
Limiting iBEP	6.8	9.8	16.5	22.5	1.6E-04	2.088
Torrance	2	9	14.5	21	1.0E-03	3.985
Two mode	$-\infty$	10	15	19	3.4E-03	4.266
Lagrange	3.9	7.8	14.5	20.9	1.0E-03	4.011
One mode ($\rho = 40$)	7	10	15	22.5	3.9E-04	3.652

Table 2.5(c): switching levels (in dB) and resultant performances from the

five methods. Average SNR=15dB; $P_{th} = 10^{-3}$

	s1	s2	s3	s4	P_{avg}	B_{avg}
Limiting iBEP	6.8	9.8	16.5	22.5	1.6E-04	2.088
Torrance	3	6	15	22	1.6E-03	2.570
Two mode	2	9	14	18	5.2E-03	2.905
Lagrange	4.3	8.1	14.8	21.2	1.1E-03	2.534
One mode ($\rho = 77$)	4	7	12	20	5.5E-03	3.073

In chapter 4, some further simulations applying these switching levels
for adaptive modulation in practical communication systems will be made.

Chapter 3

Introduction to IEEE 802.16 SCa

In recent years, interest in Broadband wireless access (BWA) systems has greatly increased. Some benefits such as easy maintainability and portability of the wireless communication systems make BWA systems an attractive alternate to cable or digital subscriber line (DSL) in the "Last Mile" application. To compete with the wired counterparts, BWA systems have to offer similar high data rates of tens of megabits per second.

The Institutes of Electrical and Electronics Engineers Standard Association (IEEE-SA) developed IEEE Standard 802.16 [7][8], which specifies the WirelessMAN Air Interface for wireless metropolitan area networks. IEEE 802.16 addresses the "first-mile/last-mile" connection in wireless metropolitan area networks. It focuses on efficient use of bandwidth between 10 and 66 GHz. For different frequency band of use, it defines a medium access control (MAC) layer that supports multiple physical layer specifications.

3.1 Background

The IEEE 802.16 Task Group a developed IEEE Standard 802.16a [9], which amends IEEE Std 802.16. It enhances medium access control layer and provides additional physical layer for frequency band between 2 and 11

GHz, where NLOS channel condition often occurs and multi-path effect may be severe. Its MAC layer is also capable of supporting multiple physical layers optimized for the frequency band used. There are three system modes in 802.16a: SC (single carrier), OFDM, and OFDMA. In the most of the following, single carrier mode will be mainly considered.

Because of the property of low complexity to equalize a severe multi-path fading channel, OFDM techniques have been adopted in many wireless applications such as WLAN and DVB. However, some problems in OFDM systems such as high PAPR (Peak to Average Power Ratio) and sensitivity to phase noise are also very serious drawbacks. SC-FDE (Single Carrier with Frequency Domain Equalizer) systems [10], which perform equalization in the frequency domain, combine advantages of multi-carrier and conventional single carrier systems. They have similar ability to defend multi-path fading and complexity to OFDM systems while the high PAPR and sensitivity to phase noise problems are greatly eliminated. Besides, the conventional single carrier techniques developed in past years can be used. Principles of SC with FDE will be introduced in chapter 4.

Another important advantage to adopt FDE in 802.16 SCa is its ability to coexist with OFDM systems. Fig. 3.1 shows block diagrams for parts of OFDM and SC-FDE systems. It is clear that the most difference between two systems is the position of IFFT block. In OFDM systems, IFFT is done on the transmitter while in SC-FDE systems it is on the receiver. A communication system containing the two modes can be implemented by switching the IFFT block between the transmitter and receiver. When OFDM mode is used, IFFT block is switched to the transmitter and when SC-FDE mode is used, it is switched to the receiver.

OFDM

Figure 3.1: OFDM and SC-FDE systems

Figure 3.2: Transmitter structure of 802.16-SCa PHY layer

3.2 System Structure

The 802.16 SCa is based on single carrier technology and designed for NLOS environment for 2-11G frequency bands. The transmitter structure for both UL (uplink) and DL (downlink) is shown in Fig. 3.2. The source bits are first randomized, and then channel coded and mapped to QAM symbols. Suitable FEC and modulation type is chosen according to the channel condition. The QAM symbols will be then framed to a burst and some framing symbols will be added. Then the burst-framed symbols will be multiplexed into a duplex frame that may contain multiple bursts. The I component and Q component will be passed to their own pulse shaping filters. After quadrature modulating to the carrier frequency, power control will be done such that proper output power is transmitted. The function of the blocks in Fig. 3.2 will be introduced in the following sections.

3.3 Channel coding and modulation

3.3.1 Source Bit Randomization

The transmitted source data are first randomized before channel coding for energy dispersal. The randomization is performed with the output of the Linear-Feedback Shift Register (LFSR), which have the characteristic polynomial $1+X^{14}+X^{15}$, as shown in Fig. 3.3. The randomizer should be re-initialized at the start of each burst with the sequence: (msb) 1 0 0 1 0 1 0 1 0 0 0 0 0 0 0 (lsb). The transmitted source data enter the randomizer sequentially and combine with the randomization bits in a XOR operation. In the receiver, the same randomizer with the same initial sequence is used to recover the source data bit. Only source bits are randomized, while
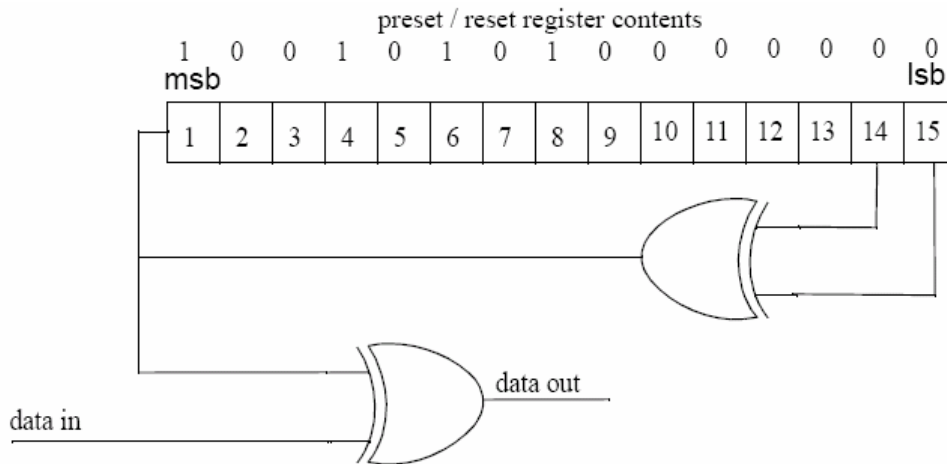
framing elements and pilot symbols are not.

Figure 3.3: LFSR for data randomization (from [9])

3.3.2 FEC and QAM constellation mapping

There are four FEC types defined in 802.16a. They are "concatenated FEC", "No FEC", "Block Turbo Codes", and "Convolutional Turbo Codes", and the last two are optional. For broadcast messages, QPSK and "concatenated FEC" with a rate 1/2 convolutional inner code is used. For non-broadcast messages, adaptive modulation and "concatenated FEC" will be support, and support of "Block Turbo Codes" and "No FEC" is optional. While omitting FEC, error control relies only on ARQ mechanisms.

In the No FEC option, source data will be mapped directly to a QAM symbol constellation, using Gray encoding. These maps for BPSK, QPSK, 16-QAM, and 64-QAM are shown in Fig. 3.4. No FEC operation is mandatory for QPSK, and optional for other modulation methods.
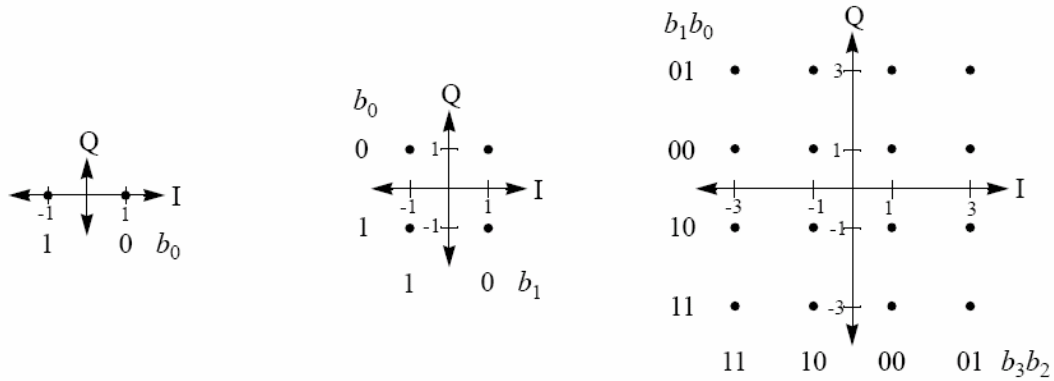
Figure 3.4(a): Gray maps for BPSK, QPSK, and 16-QAM constellations
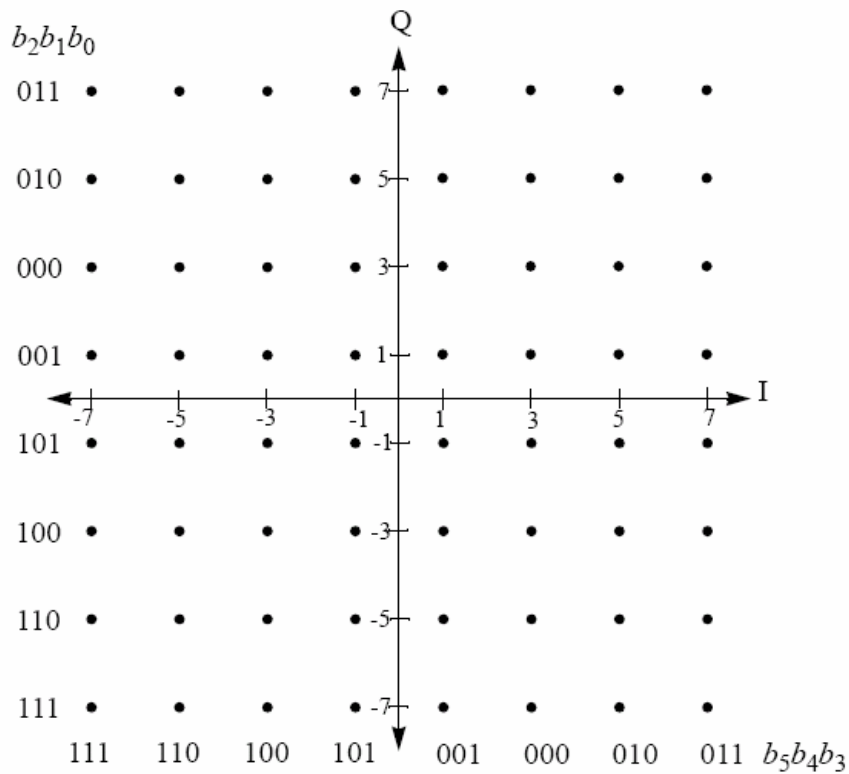
Figure 3.4(b): Gray maps for 64-QAM constellation

3.4 Burst framing

A burst consists of three components, which are burst preamble, payload and RxDS interval, as in Fig. 3.5.
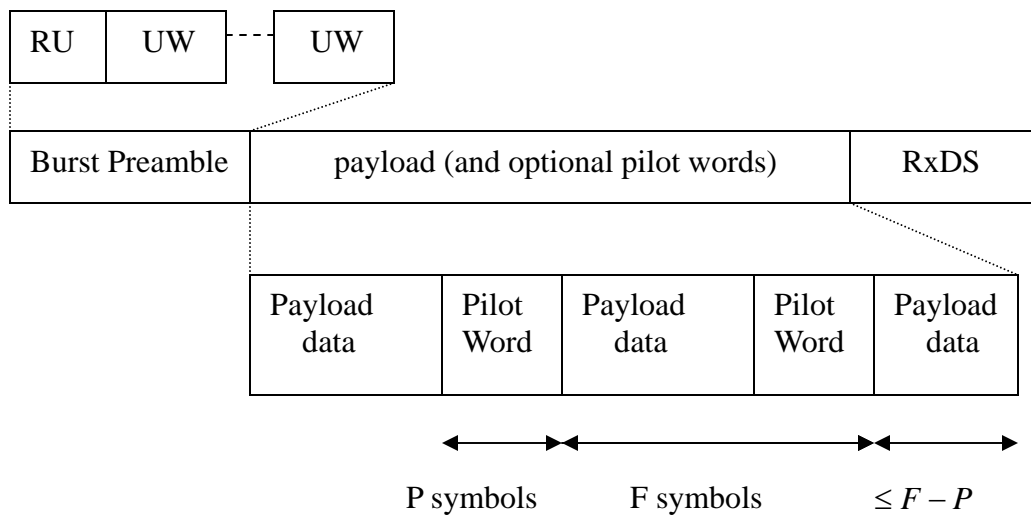
Figure 3.5: Burst composition

3.4.1 Burst preamble

A burst preamble consists of a RU (ramp up) region and multiple UW (unique word). Burst profile parameters should specify R_r, the length of ramp up region, U, the number of symbols in a unique word, and m, the number of unique words in one burst preamble.

The ramp up region is constructed by the last R_r symbols in a unique word. According to different U values, Frank-Zadoff or Chu sequences are chosen as unique words. Both the two sequences possess CAZAC (Constant Amplitude Zero [periodic] Auto-Correlation) properties. The sequence length $U = 64$ is considered as default setting. For symbol rates below 1.25 M symbols/s $U = 16$ and for symbol rates above 20 M symbols/s $U = 256$ should be supported separately. In Table 3.1, sequence types for different length of U are shown. The other length of unique word may be useful for

longer or shorter delay spread channels.

Table 3.1: Unique Word lengths, types, and support status

Length, U (symbols)	Sequence type	Support status
0	-	Optional
8	Chu	Optional
16	Frank-Zadoff	Mandatory below 1.25Msym/s
32	Chu	Optional
64	Frank-Zadoff	Mandatory(default)
128	Chu	Optional
256	Frank-Zadoff	Mandatory below 20Msym/s
512	Chu	Optional

Unique word sequence should be generated from

$$I[n] = \cos(\theta[n])$$
$$Q[n] = \sin(\theta[n]) \tag{3.1}$$

For a Chu sequence:

$$\theta[n] = \theta_{chu}[n] = \frac{\pi n^2}{U} \tag{3.2}$$

and for a Frank-Zadoff sequence:

$$\theta[n] = \theta_{frank}[n]$$
$$\theta_{frank}[n = p + q\sqrt{U}] = \frac{2\pi pq}{\sqrt{U}} \tag{3.3}$$
$$\text{where } p = 0,1,...,\sqrt{U} - 1$$
$$q = 0,1,...,\sqrt{U} - 1$$

For $U = 16$, 64, and 256 (Frank-Zadoff case), the sequences are composed symbols from M-PSK alphabets. On the other hand, for $U = 8$, 32, 128, and 512 (Chu case) the sequences are derived from a special class of

alphabet called polyphase symbol alphabets and require additional care in hardware implementation.

3.4.2 Burst payload

The burst payload block contains payload data, and may also contain inserted Pilot Words periodically, as in Figure 3.5. Pilot Words are blocks composed of an integer $n \geq 0$ multiple of unique words. The number of Pilot Words n and the period of Pilot Words F are also specified in the burst profile. The data payload can be of any arbitrary length.

When there are Pilot Words inserted in the payload, F must be constant. As in the figure, Pilot Word patterning should cease when $F - P$ or less payload data remain in the burst.

3.4.3 Null payload fill

Null payload is used to fill a burst frame if needed. It uses the null fill data type defined as zero-valued source bits after randomization and mapped to QPSK symbols using Gray code mapping in Fig. 3.4(a). The transmit power can be lowered during null payload transmission period.

When the channel condition is bad and average received SNR is low, we can use the null fill data type which corresponds to "no transmission" mode in chapter 2. Thus the five mode adaptive modulation switching levels in chapter 2 can be directly applied.

3.4.4 RxDS (Receiver delay spread clearing region)

The RxDS interval is a quiet period for the transmitter to ramp down, and for

the receiver to collects delay-spread versions of symbols at the end of the payload. The length of the RxDS is always the same with the length of a unique word, if it is not suppressed.

3.5 Duplex framing

Both FDD (Frequency Division Duplex) and TDD (Time Division Duplex) operations can be used in 802.16. In FDD mode, burst transmission or continuous transmission can be chosen, where the latter is a special case of the former. Figure 3.6 shows an example of a FDD burst downlink sub-frame. A downlink burst cannot exceed the length of a downlink sub-frame, but need not fill the entire sub-frame. There may be multiple downlink bursts within a downlink sub-frame, and in the example there are two bursts in a sub-frame.

| BP | FCH | DL payloads | RxDS | BP | DL payloads | RxDS |

DL sub-frame(n)

UL sub-frame(n-1)

| Requests | UL payloads |
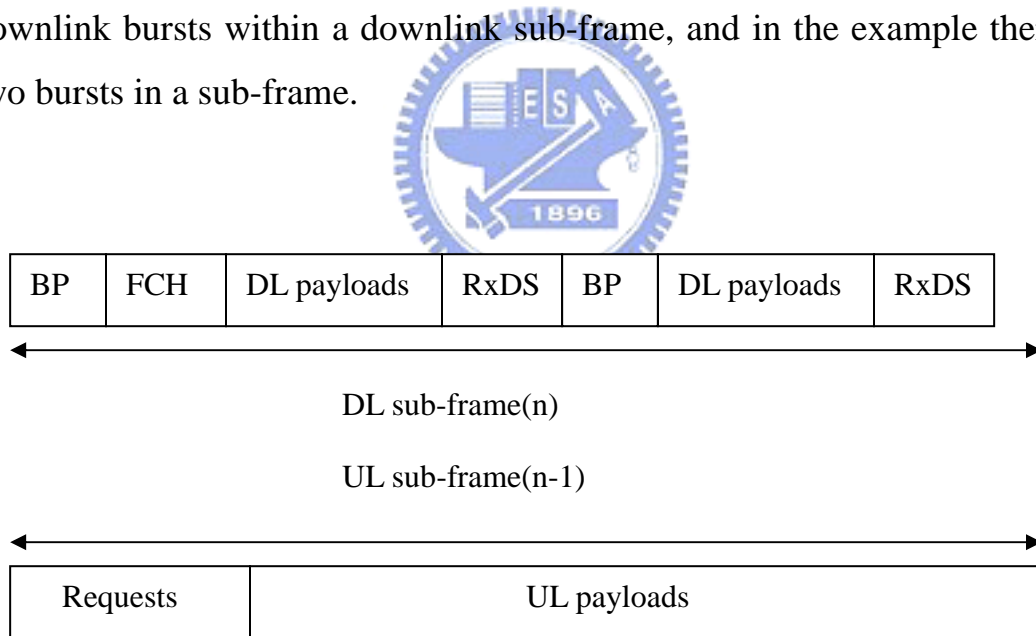
Figure 3.6: Example of FDD with burst DL

A continuous DL can be derived from a burst DL. To do so, the RxDS and ramp-up regions should be suppressed and instead of null payload filling.

Also, when a continuous DL has no enough data to fill a MAC frame, null payload should be inserted. An example of continuous DL transmission is shown in Fig. 3.7.

UW	UW	FCH	DL payloads	UW	UW	DL payloads

Preamble 1   Payload 1   Preamble 2   Payload 2
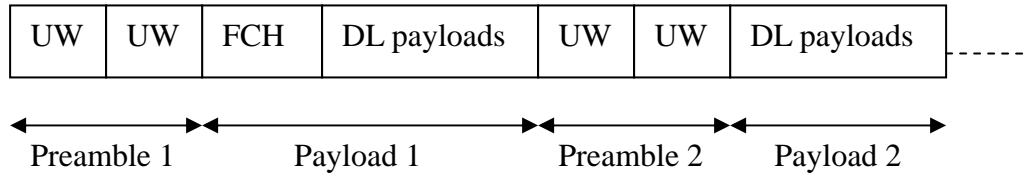
Figure 3.7: Example of continuous mode DL transmission

For both FDD and TDD modes, the first burst in each DL sub-frame will commences with a burst preamble (BP), and directly followed by a frame control header (FCH). The FCH segment is a broadcast payload containing DCD (Downlink Channel Descriptor), UCD (Uplink Channel Descriptor), and MAPs. Among them, DCD messages contain downlink burst profiles, which define the parameters used in the bursts. Only the first burst in the sub-frame contains the FCH.

Table 3.2: Burst profile settings for DL burst containing BCH

burst profile parameter	Default setting	Alternatives
Modulation type (FCH payload only)	QPSK; Concatenated FEC without block interleaving	-
Inner (CC) code rate (FCH payload only)	1/2	-
Preamble length	length=$mU + R_r$ symbols; $m = 3$ repeated UWs; $R_r = 4$ ramp symbols	$2 \leq m < 11$; $0 \leq R \leq \dfrac{U}{2} \leq 60$ in increments of 4 symbols
Unique Word length	$U = 64$ symbols	$U = 16, 256$ (optional for some symbol rate)
Pilot Word parameters	$n = 0$ repeated UWs $F = 256$ symbol interval	$n = 1, 2$; $F = 256$(when $U \neq 256$), $F = 1024$

Bursts containing FCH segment use FEC with rate 1/2 QPSK inner convolutional code and RS outer code. The inner convolutional code should be zero-state terminated at the end of the FCH segment. Table 3.2 shows some burst profile settings for downlink burst containing broadcast FCH. Burst profiles for non-broadcast messages are adaptive and specified by the MAC management.

3.6 Baseband Pulse Shaping and Quadrature Modulation

In this stage, I and Q signals are filtered by square-root raised cosine filters. The default roll-off factor is $\alpha = 0.25$. $\alpha = 0.15$ and 0.18 are optional. The frequency domain transfer function of the ideal square-root cosine is:

$$H(f) = \; 1 \qquad\qquad\qquad \text{for } |f| < f_N(1-\alpha)$$

$$= \sqrt{\frac{1}{2} + \frac{1}{2}\sin\left(\frac{\pi}{2f_N}\left[\frac{f_N - |f|}{\alpha}\right]\right)} \quad \text{for } f_N(1-\alpha) \le |f| < f_N(1+\alpha) \qquad (3.4)$$

$$= \; 0 \qquad\qquad\qquad\quad \text{for } |f| \ge f_N(1+\alpha)$$

where $f_N = \dfrac{1}{2T_s} = \dfrac{R_s}{2}$, f_N is the Nyquist frequency, T_s is the symbol duration

and R_s is the symbol rate.

    An FIR Raised cosine filter may be synthesized directly from the impulse response, which is:

$$h(t) = \frac{4\alpha}{\pi\sqrt{T}} \frac{\cos\left(\dfrac{(1+\alpha)\pi t}{T}\right) + \dfrac{T}{4\alpha t}\sin\left(\dfrac{(1-\alpha)\pi t}{T}\right)}{1 - \left(\dfrac{4\alpha t}{T}\right)^2} \qquad (3.5)$$

    After pulse shaping, what follows is quadrature modulation. Let $I(t)$ and $Q(t)$ be the filtered baseband signals of I and Q symbols. Then the quadrature modulated transmit waveform is:

$$s(t) = I(t)\cos(2\pi f_c t) - Q(t)\sin(2\pi f_c t) \qquad (3.6)$$

where f_c is the carrier frequency.

Chapter 4

Simulation Result

Adaptive modulation techniques will be applied to 802.16-SCa systems over wireless narrowband and broadband channels in this chapter. First, we will introduce some suitable equalization techniques to equalize a frequency selective fading channel. Then performance of different adaptive modulation methods on flat and frequency-selective channels will be considered and compared.

4.1 Equalization techniques

4.1.1 Basic

It had been mentioned that in the NLOS environments, multi-path effect can be severe. Since the target data rate is high, convention equalization in the time domain will have very high complexity. For example, assume that time dispersion is 5μs and symbol rate is 10MHz, then the caused ISI will over more than 50 symbols. In this case, a time domain equalizer should be of 100 to 200 taps to be sufficient to reduce ISI. Such a high complexity time domain equalizer can't be realized in practical. In 802.16 SCa, data are transmitted in blocks of length F so that frequency domain equalization whose complexity closes to OFDM systems can be used.

Transmitter

| QAM modulator | → | Add cyclic prefix | → | Radio channel | → |

Channel estimation

Receiver

| Remove Cyclic prefix | → | FFT | → | Equalizer | → | IFFT | → | QAM demodulator |

Frequency domain equalizer
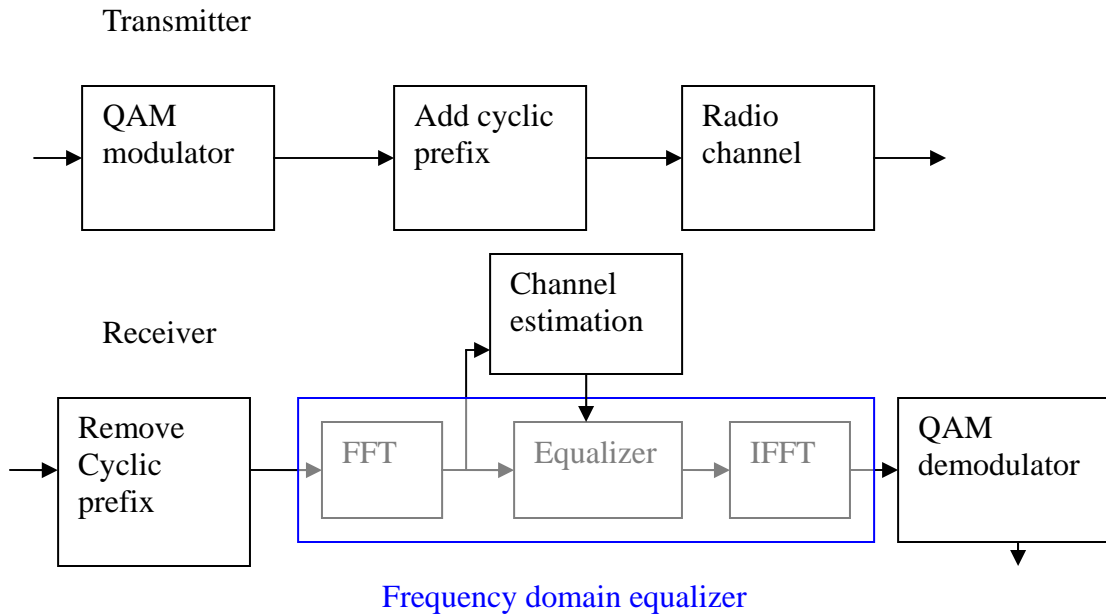
Figure 4.1: Block diagram of a transceiver adopting FDE

| CP1 | | CP1 | CP2 | | CP2 |

P   Data block
           M (FFT size)
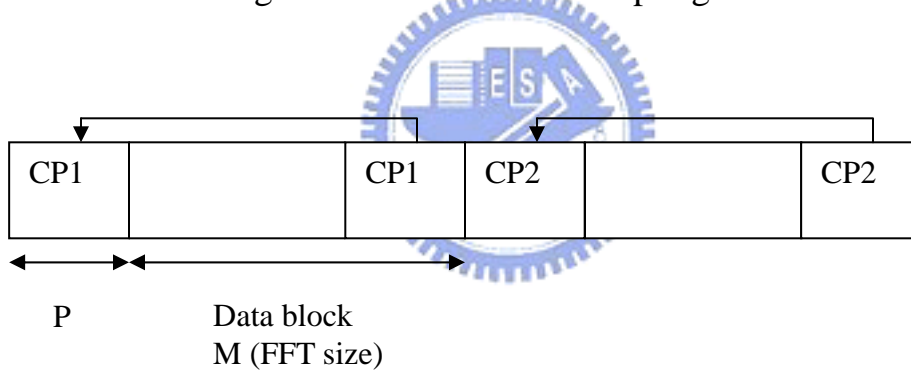
Figure 4.2: Example of transmitted data structure using a cyclic prefix

Figure 4.1 shows a basic structure of a transceiver using frequency domain linear equalization. The last P symbols in the transmitted block are reproduced and used as cyclic prefix adding in front of the block, as in Figure 4.2. As in OFDM systems, the cyclic prefix is added to remove the effect of inter-block interference. The length of the cyclic prefix has to exceed the maximum expected length of the channel impulse response. Because of the cyclic extension of the transmitted block, the convolution of

the block and the channel impulse response can be calculated by circular convolution of the corresponding samples. In frequency domain, it can be written as:

$$R(nf_0) = H(nf_0)S(nf_0) + N(nf_0)$$
$$n \in Z \; ; \; f_0 : \text{sampling frequency}$$

(4.1)

In the equation, $R(f)$, $H(f)$, and $S(f)$ are Fourier transforms of the received data block $r(t)$, channel impulse response $h(t)$, and the original transmitted data (not including cyclic extension) block $s(t)$. $N(f)$ is the Fourier transform of the noise.
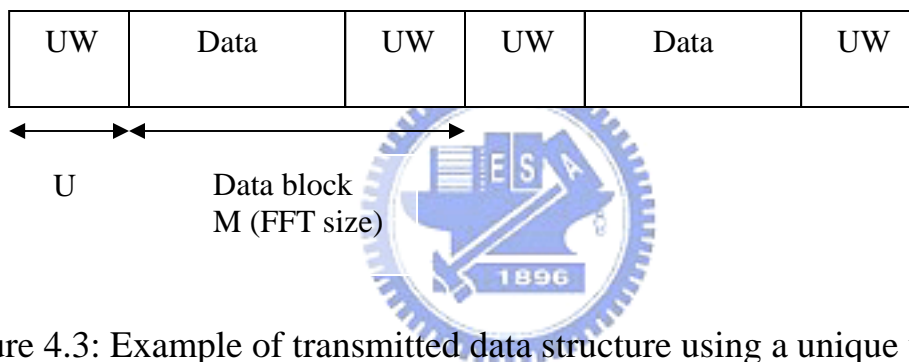
Figure 4.3: Example of transmitted data structure using a unique word

The existence of cyclic prefix obviously introduces some overhead. If we replace the cyclic prefix with some know sequences, the overhead could be used in other purposes such as synchronization and channel estimation. In Fig. 4.3, transmitted data structure using a Unique Word instead of cyclic extension is shown. Two popular Unique Words, Frank-Zadoff and Chu sequences are introduced in chapter 3. For channel estimation purpose, at least two adjacent unique words are required. Fig. 4.4 shows data structure with smallest number of unique words for burst mode and continuous mode transmission respectively. The shaded unique words are for channel estimation, and those preceding them act as cyclic prefix and shield the

shaded unique words from the inter-symbol interference from previous data. For decision feedback equalizers, an additional advantage using unique words is to prevent error propagation beyond one FFT block since the last symbols (UWs) in each block are known.
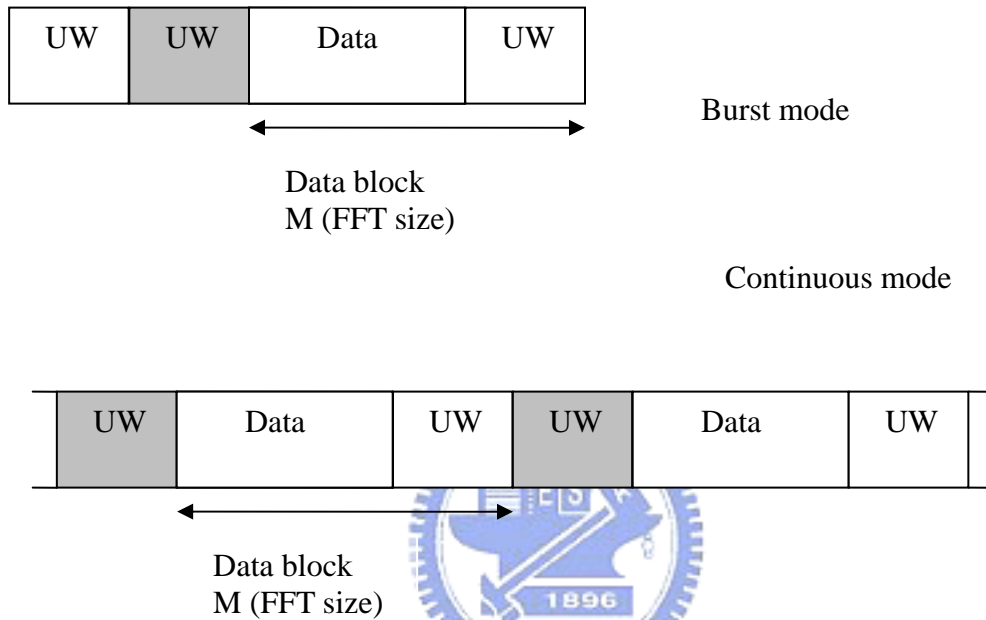
Figure 4.4: Burst and continuous transmissions using unique words
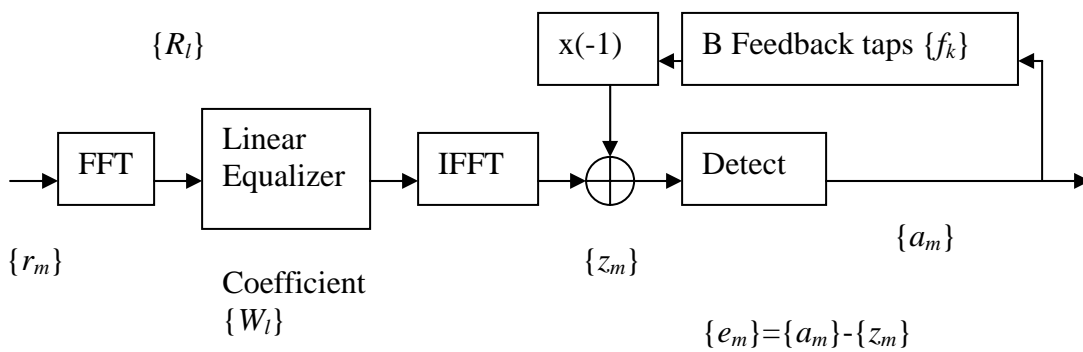
Figure 4.5: Frequency domain decision feedback equalizer model

4.1.2 Least Square Minimization

Now consider the receiver structure using a decision feedback equalizer in Fig. 4.5. Precisely speaking, the equalizer should be classified to the hybrid time-frequency domain DFE approach since the conventional transversal filtering is used for the feedback part.

The equalizer coefficients $\{\tilde{W}_l\}$ and $\{\tilde{f}_k\}$ can be estimated during the training blocks by LS (Least Square) algorithm. The algorithm finds the solution minimizing the sum of squared errors. Details of the algorithm can be found in Appendix A, and only results are shown here.

Let $\{a_m ; m = 0,1,...,U-1\}$ be the original time domain sequence of the training block (UW) and $\{A_l ; l = 0,1,...U-1\}$ is its FFT counterpart. Also, let $\{r_m^{(n)} ; m = 0,1,...,U-1 ; n = 0,1,...N-1\}$ is the received sequence for the nth training block and $\{R_l^{(n)} ; l = 0,1,...,U-1 ; n = 0,1,...N-1\}$ is its FFT counterpart. Then the channel is estimated in the frequency domain as $\{\tilde{H}_l = \frac{1}{N}\sum_{n=1}^{N}\tilde{H}_l^{(n)}$, where $\tilde{H}_l^{(n)} = \frac{R_l^{(n)}}{A_l}$; $l = 0,1,...,U-1 ; n = 0,1,...N-1\}$. Next the frequency domain samples are interpolated from size U to size F, which is the length of a payload block.

Let B be the number of non-zero feedback filter coefficients and F_B be the set of corresponding indices. Then $\tilde{f} = \{\tilde{f}_{k_1}, \tilde{f}_{k_2}, ..., \tilde{f}_{k_B})'$ can be derived from the following equation:

$$\tilde{f} = -\tilde{V}^{-1}\tilde{v}$$

where $\tilde{v} = (\tilde{v}_{k_1}, \tilde{v}_{k_2}, \dots \tilde{v}_{k_B})'$,

$$\tilde{V} = \begin{bmatrix} \tilde{v}_0 & \tilde{v}_{k_1-k_2} & \cdots & \tilde{v}_{k_1-k_B} \\ \tilde{v}_{k_2-k_1} & \tilde{v}_0 & \cdot & \cdot \\ \vdots & \cdot & \ddots & \cdot \\ \tilde{v}_{k_B-k_1} & \cdot & \cdot & \tilde{v}_0 \end{bmatrix} , \tag{4.2}$$

$$\tilde{v}_k = \sum_{l=0}^{F-1} |A_l|^2 \left[1 - |\tilde{H}_l|^2 \tilde{U}_l^{-1}\right] \exp(-j2\pi \frac{lk}{F})$$

and $\tilde{U}_l = \dfrac{1}{N}\sum_{n=1}^{N} |\tilde{H}_l^{(n)}|^2$

After $\tilde{f}$ is estimated, $\{\tilde{W}_l \; ; \; l = 0,1,\dots F-1\}$ can be estimated from:

$$\tilde{W}_l = \frac{\tilde{H}_l^*}{\tilde{U}_l}\left[1 + \sum_{k \in F_B} \tilde{f}_k^* \exp(-j2\pi \frac{lk}{F})\right] \tag{4.3}$$

The complexity of the equalizer increases greatly as the number of feedback coefficients B increases. Note that the $B = 0$ case corresponds to linear equalization.

4.2 Simulation on flat fading channel

The flat fading channel, which means only one path in the channel impulse response, is considered in this section. To be a contrast to adaptive modulation systems, BER performance of non-adaptive system is shown in Figure 4.6. From the figure, the average SNR needed for BPSK, QPSK, 16-QAM, and 64-QAM to achieve the target BER 10^{-3} are about 23dB, 26dB, 33dB, and 37dB respectively.
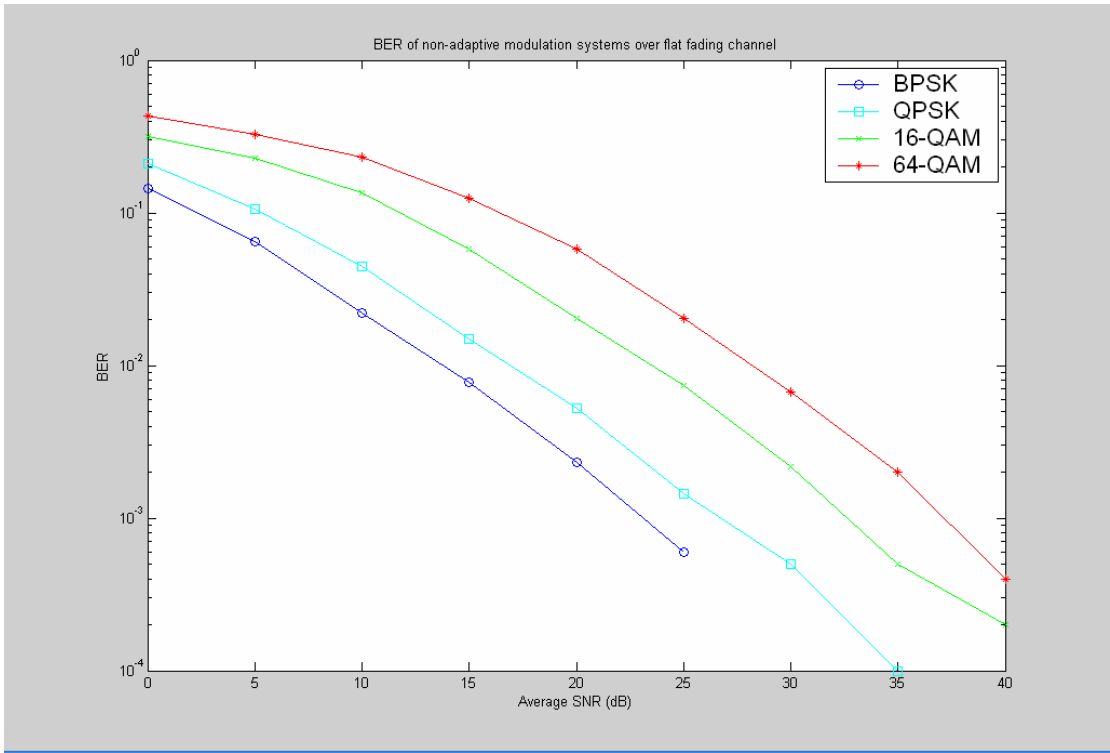
Figure 4.6: BER of various QAM systems over Rayleigh fading channel
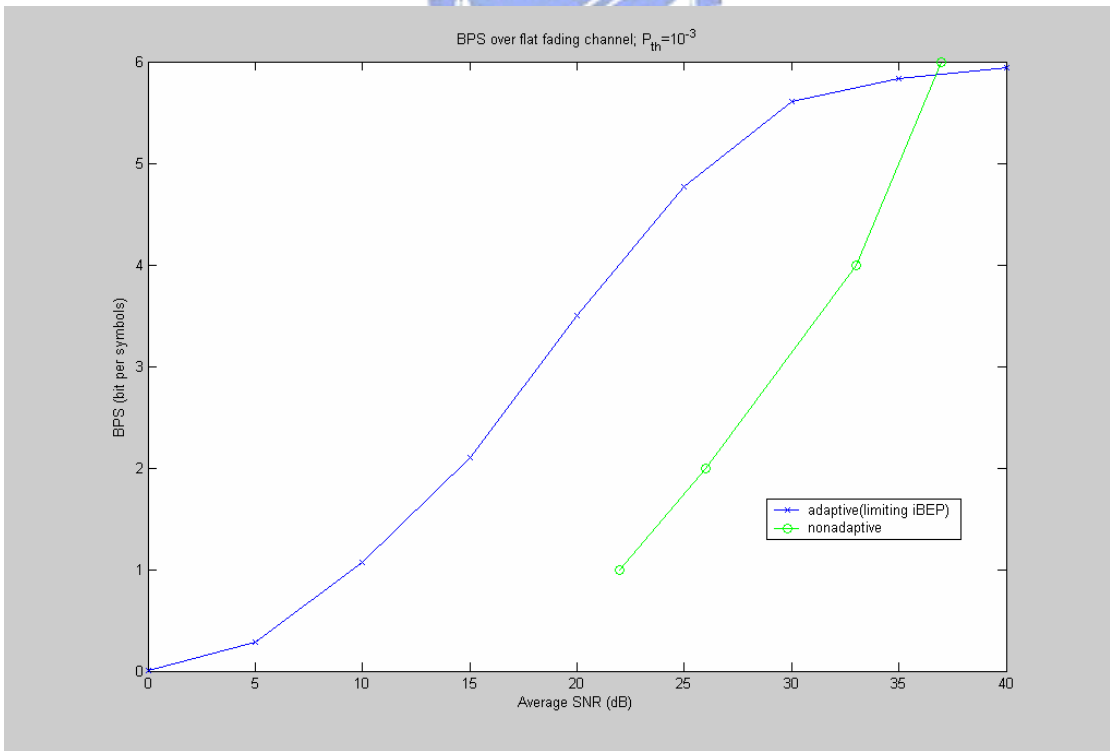
Figure 4.7: Throughput performances of adaptive and non-adaptive systems
over flat fading channel

Now consider adaptive modulation case. Figure 4.7 shows the throughput performance in BPS of adaptive and non-adaptive schemes. It's obvious that adaptive modulation system has a large improvement in throughput performance comparing to non-adaptive one over fading channel.

The BER performance of adaptive modulation system employing limiting iBEP to determine switch levels (equation 2.6) are shown in Figure 4.8 and 4.9, for target BER=10^{-3} and 10^{-2}, respectively. As described in chapter 2, the limiting iBEP method ensures at each moment the instantaneous BER is smaller than target BER, and thus the average BER is often smaller than the target BER by some amount. To further increase the throughput, switching levels determined by Lagrange method can be used, the BER performances of Lagrange method are shown in Figure 4.10 and 4.11. From the two figures, the BER performances are almost perfectly matched to the wanted target, the only exception is when the average SNR is so large that even the least robust modulation mode is always used the BER still lower than P_{th}. The above condition corresponds to that all switching levels are set to 0 ($-\infty$ dB). Throughput performances for adaptive modulation systems employing Lagrange method (equation 2.8) are shown in Figure 4.12 and 4.13. It can be seen that Lagrange method outperforms limiting iBEP method in BPS performance, while the BER is still about target BER.
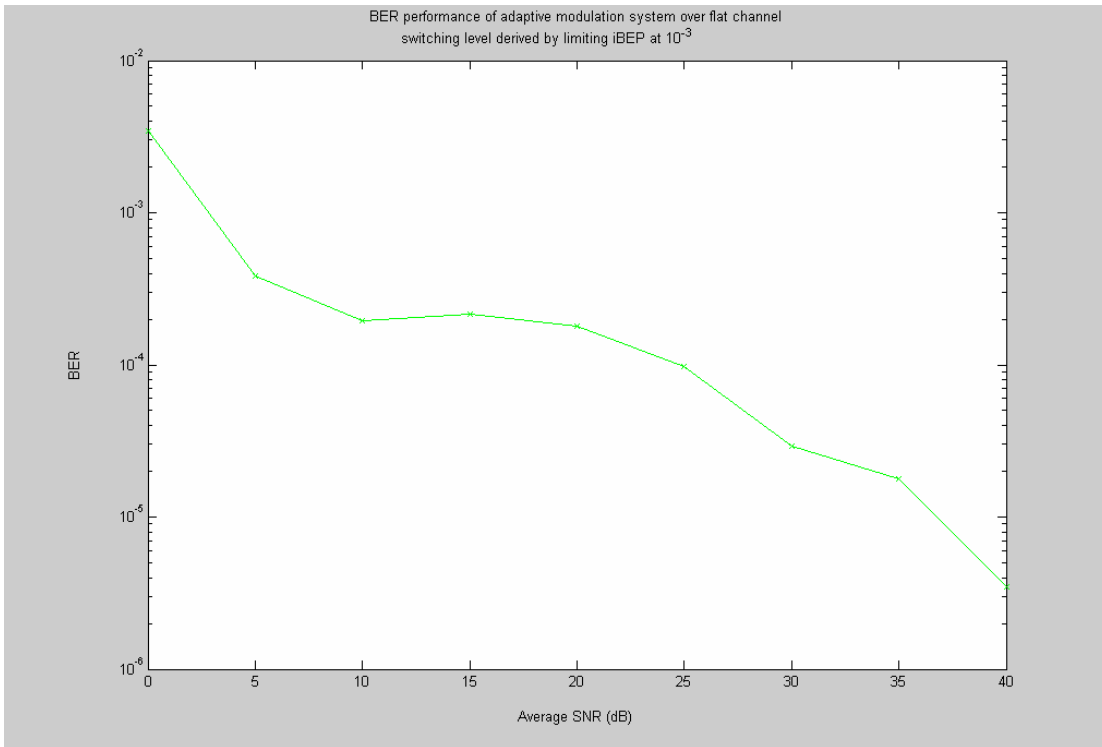
Figure 4.8: BER performance of adaptive modulation system over flat fading channel (limiting iBEP; $P_{th} = 10^{-3}$)
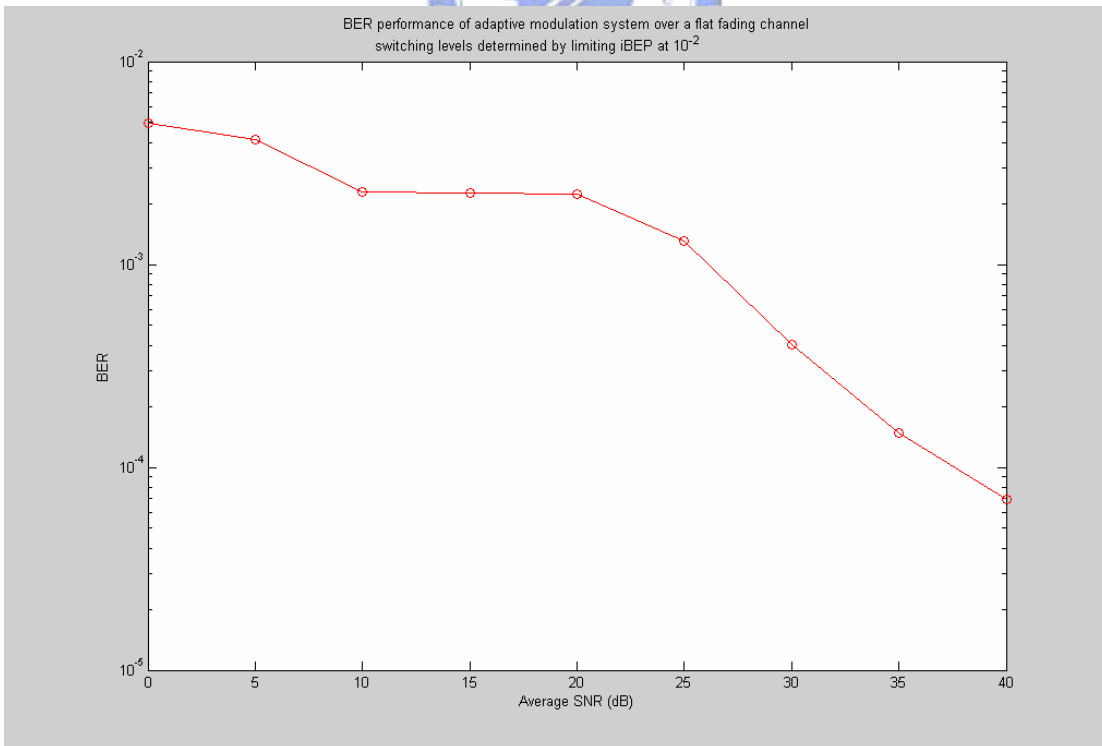
Figure 4.9: BER performance of adaptive modulation system over flat fading channel (limiting iBEP method; $P_{th} = 10^{-2}$).
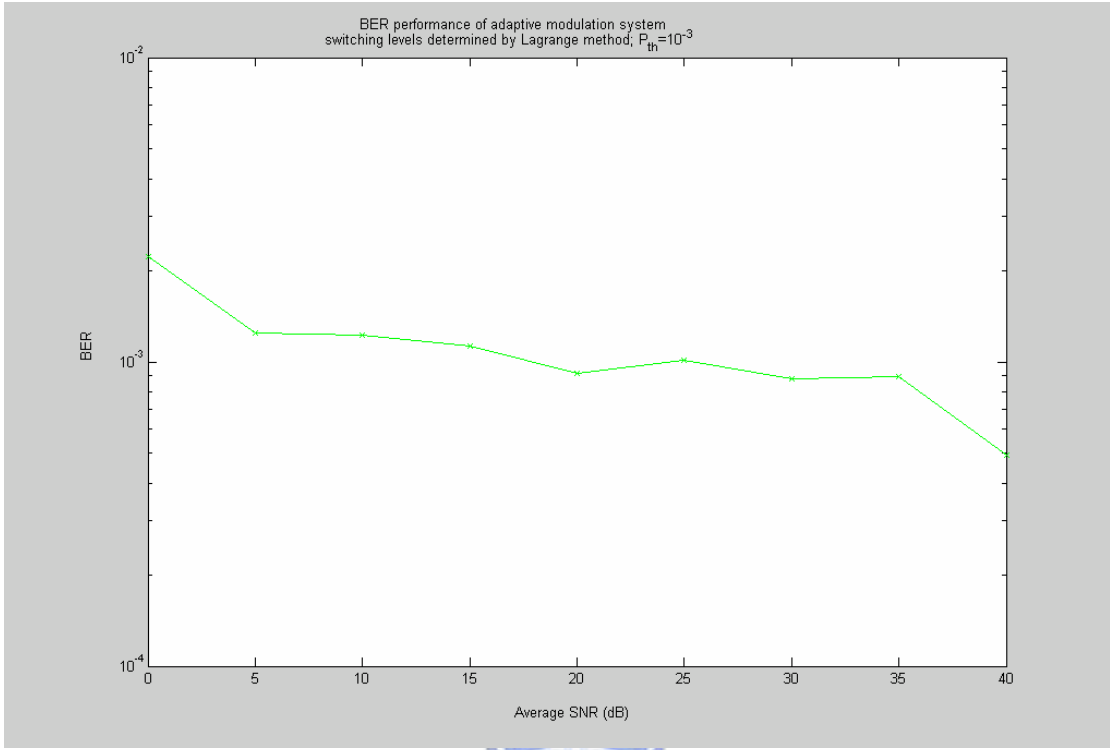
Figure 4.10: BER performance of adaptive modulation system over flat fading channel (Lagrange method; $P_{th} = 10^{-3}$).
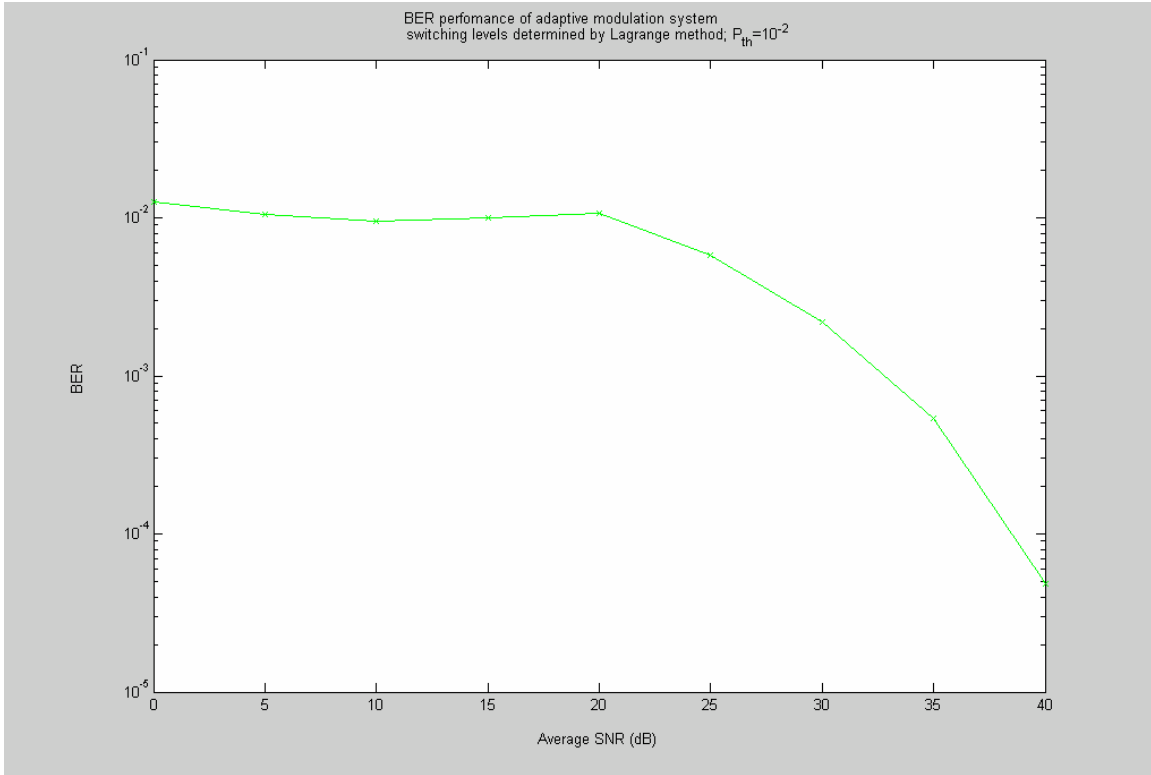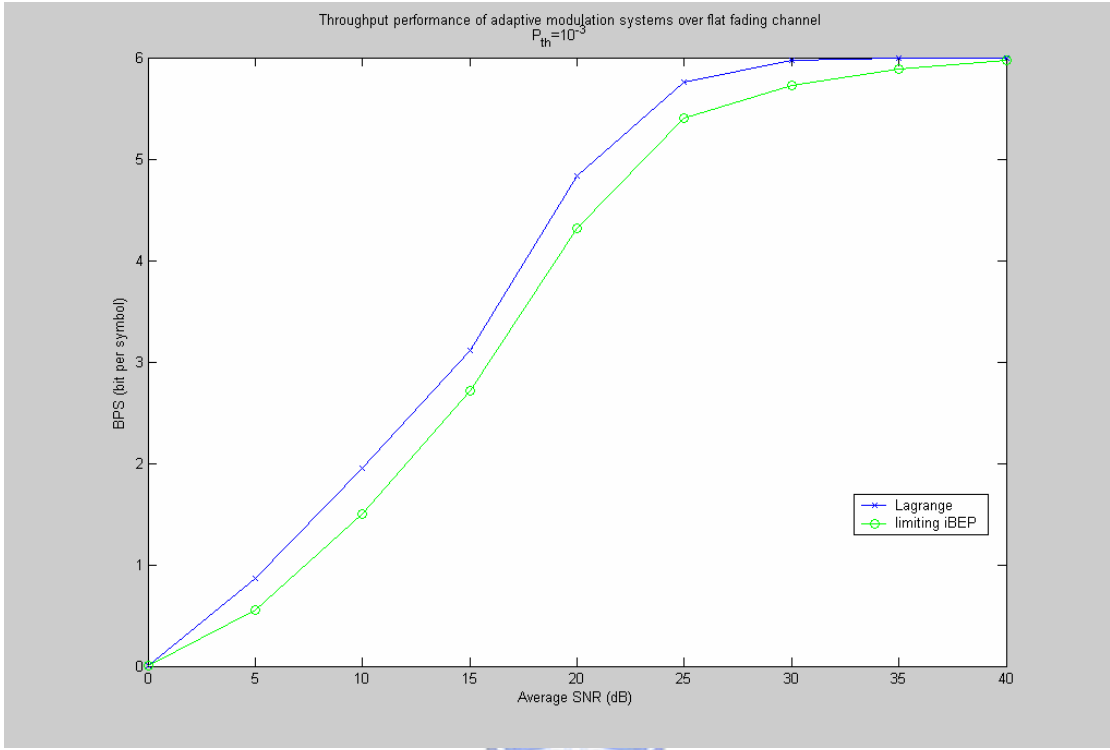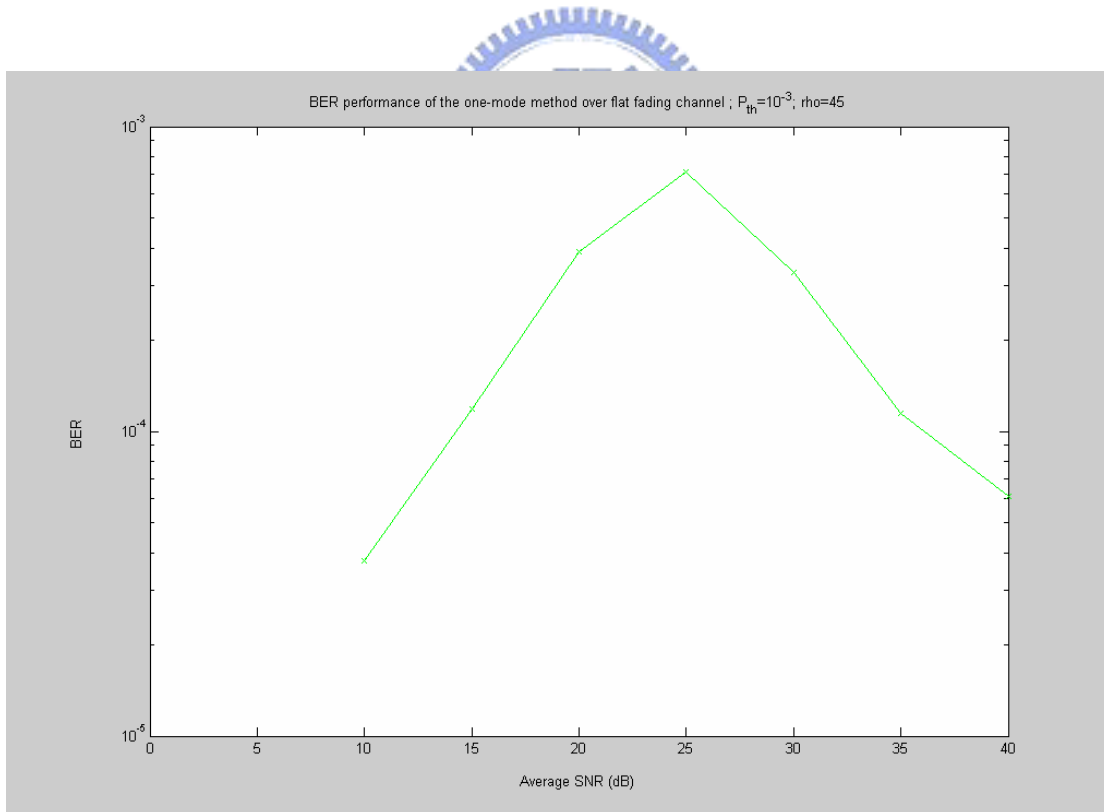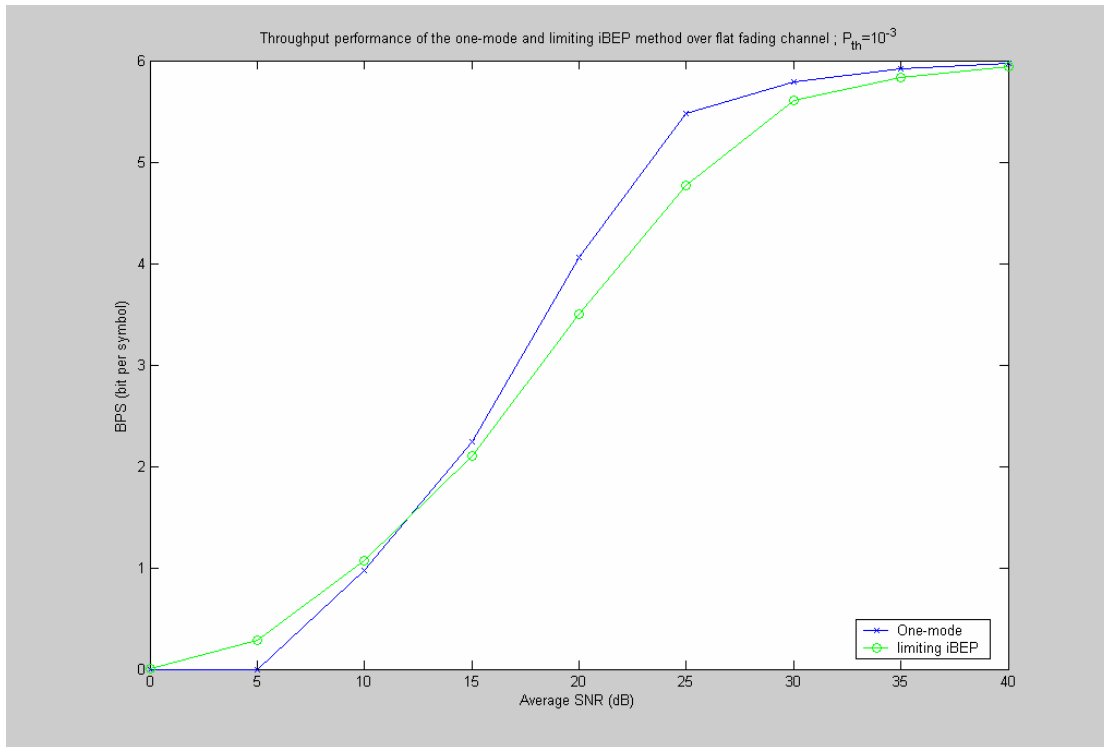
Figure 4.11: BER performance of adaptive modulation system over flat fading channel (Lagrange method; $P_{th} = 10^{-2}$).

Figure 4.12: Throughput performance of adaptive modulation system employing Lagrange method. $P_{th} = 10^{-3}$
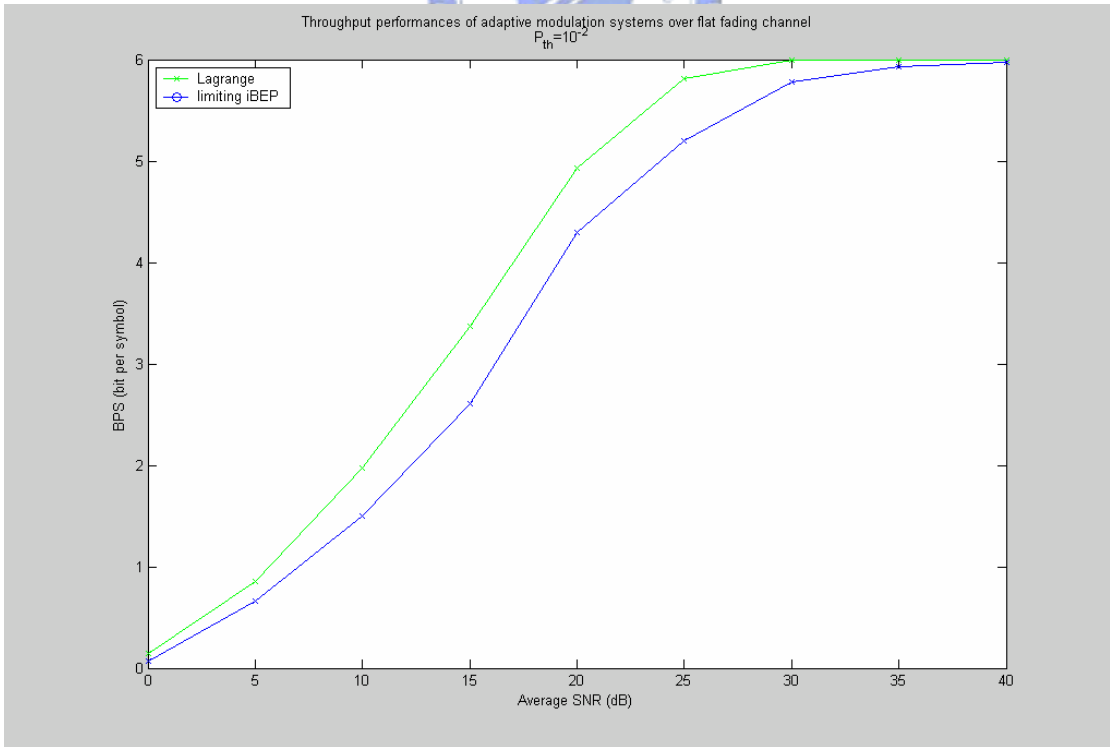
Figure 4.13: Throughput performance of adaptive modulation system employing Lagrange method. $P_{th} = 10^{-2}$

The BER and BPS performances of the one-mode method (equation 2.17) are shown in Figure 4.14 and 4.15. In this simulation the parameters are selected as $P_{th} = 10^{-3}$, $\rho=45$ (same as example in chapter 2). It can be seen the average BER of the one-mode method is usually smaller than the target BER 10^{-3}, but is closer to it than limiting iBEP method case (Figure 4.8) for the average SNR is larger than 15dB. When the average SNR is smaller than 10dB, the switching levels determined by one-mode method are too conservative, and thus almost no error occurs. Actually, from Figure 4.15, we know that the one-mode method has higher BPS than the limiting iBEP method for average SNR larger than 15dB and is converse for average SNR smaller than 15dB.

Figure 4.14: BER performance of adaptive modulation system over flat fading channel (one-mode method; $P_{th} = 10^{-3}$).

Figure 4.15: BPS performance of adaptive modulation system over flat fading channel (one-mode method; $P_{th} = 10^{-3}$).

Fig. 4.16 shows mode selection probabilities of the three schemes for $P_{th} = 10^{-3}$. We can know the proportion of modulation modes for each average SNR from the figure. As the average SNR increases, the higher-order modulation modes are selected more often. As our expectation, the limiting iBEP method is the most conservative of the three and the other methods achieve higher throughput by selecting higher-order modulation modes more often for the same average SNR condition.
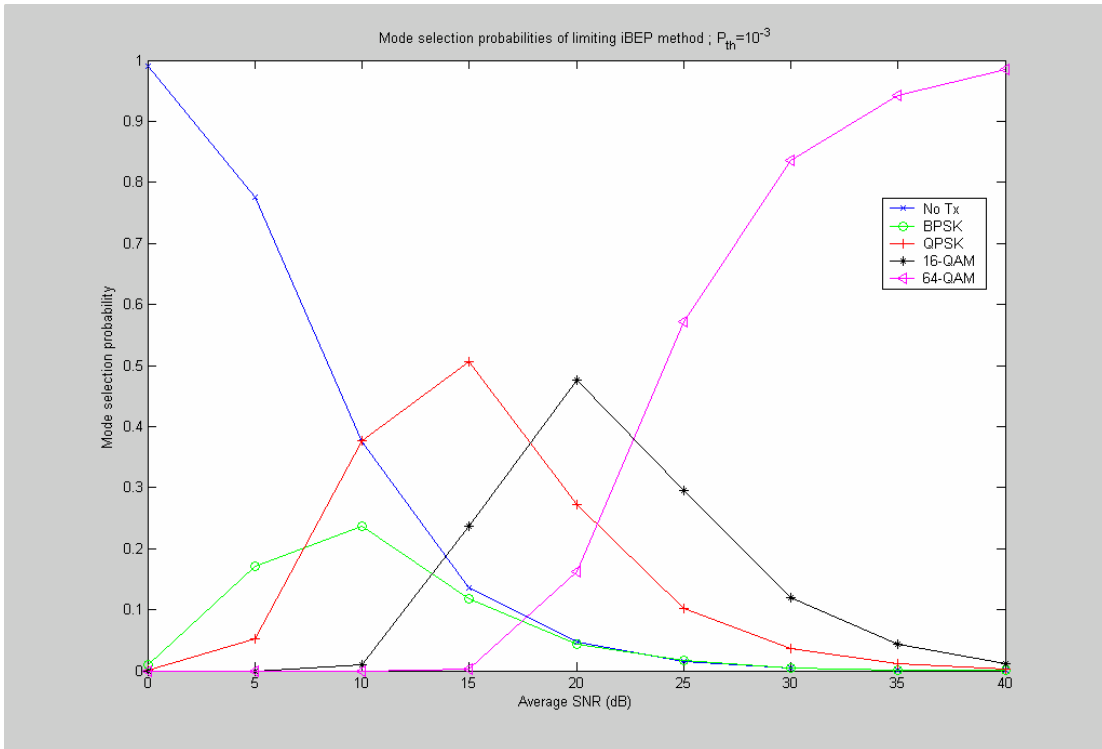
Figure 4.16 (a): Mode selection probabilities of limiting iBEP method
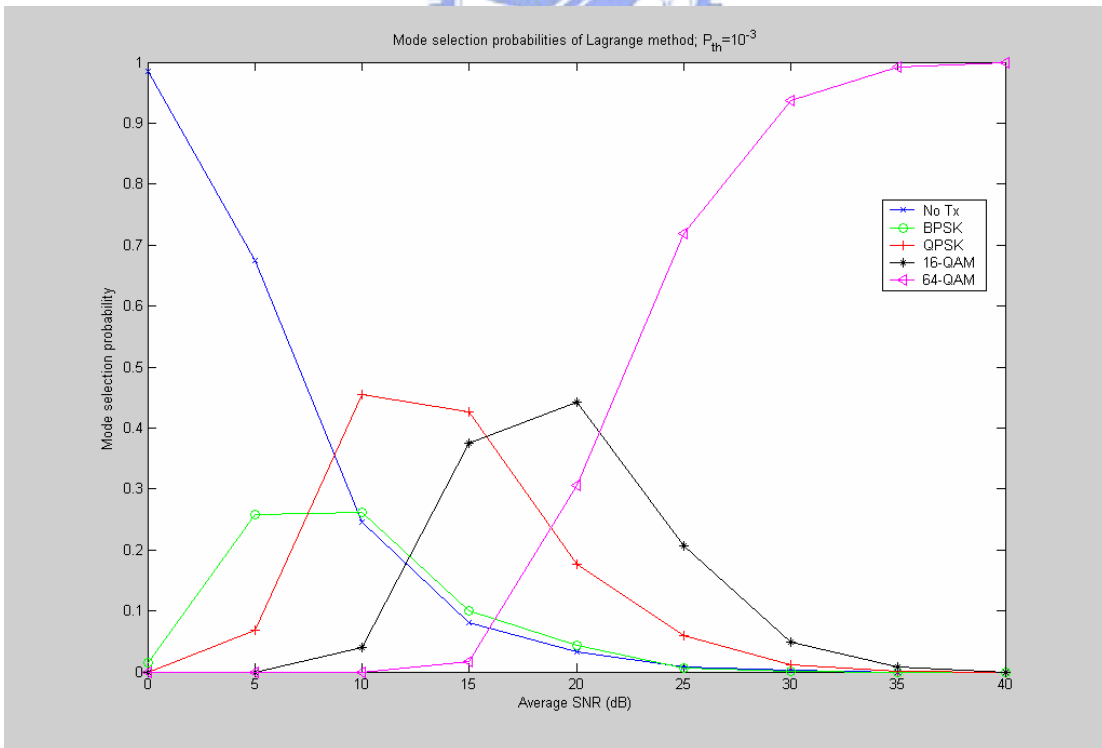
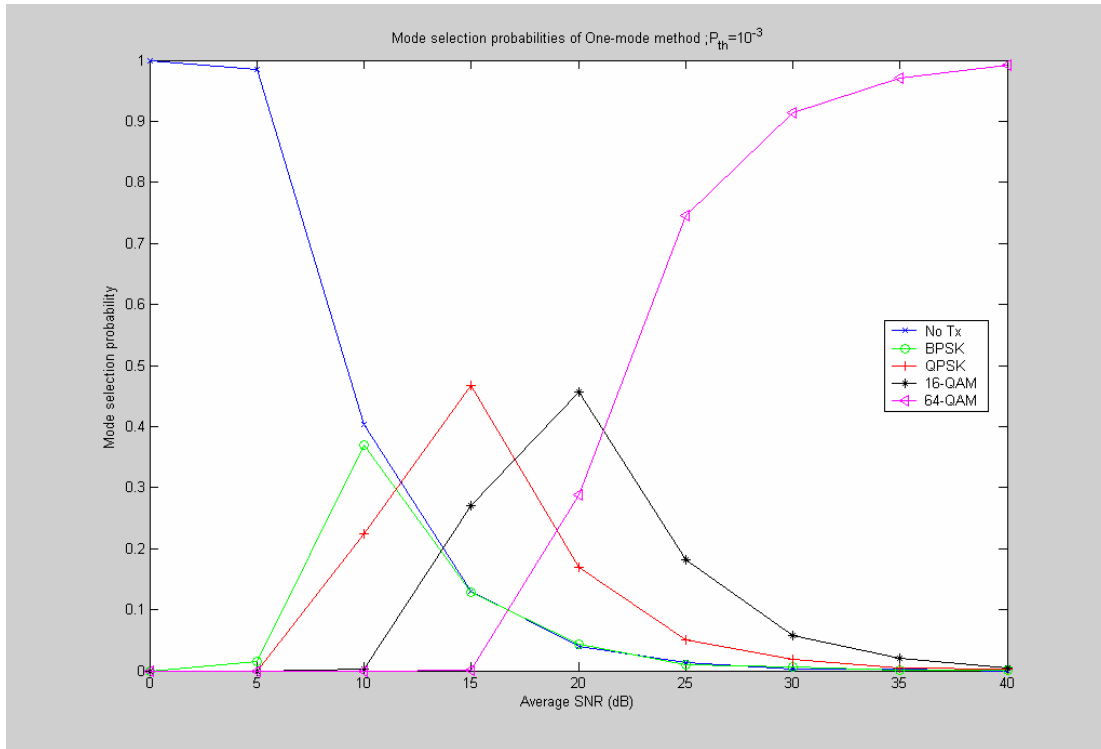Figure 4.16 (b): Mode selection probabilities of Lagrange method

Figure 4.16 (c): Mode selection probabilities of One-mode method

4.3 Simulation on frequency selective fading channel

The 802.16a standard suggests the channel models in [18]. Six channel models, which are SUI1, SUI2 … SUI6 are defined. In the following of this section, SUI4 is chosen to be the channel model to evaluate the performance gain of adaptive modulation for 802.16 SCa systems. There are three paths in the model, and each of them is Rayleigh fading and independent of one another. Table 4.1 shows some parameters of SUI-4 model. The magnitudes of the second and third paths are relative to the first path, so the total power is not unity and normalization has to be done such that total mean channel gain is 0dB.

Table 4.1: SUI4 channel model parameters

Tap	Delay(ns)	Avg power(dB)
1	0	0
2	1500	-4
3	4000	-8

System parameters used in the following simulations for multipath fading channel are shown in Table 4.2. Channel quality estimation of one burst time is assumed. The equalizers are frequency domain DFE with one nonzero feedback tap. Because of the imperfect of the equalizers, residual ISI will cause BER performance degrades for each fix-mode modulation. Thus it is inevitable that the BER of the adaptive modulation system employing switching levels optimized for flat fading channel will increase and may be larger than the target BER. In Fig. 4.17, BER comparison for limiting iBEP method, Lagrange method, and one-mode method are shown for $P_{th} = 10^{-3}$.

Table 4.2: Simulation parameters

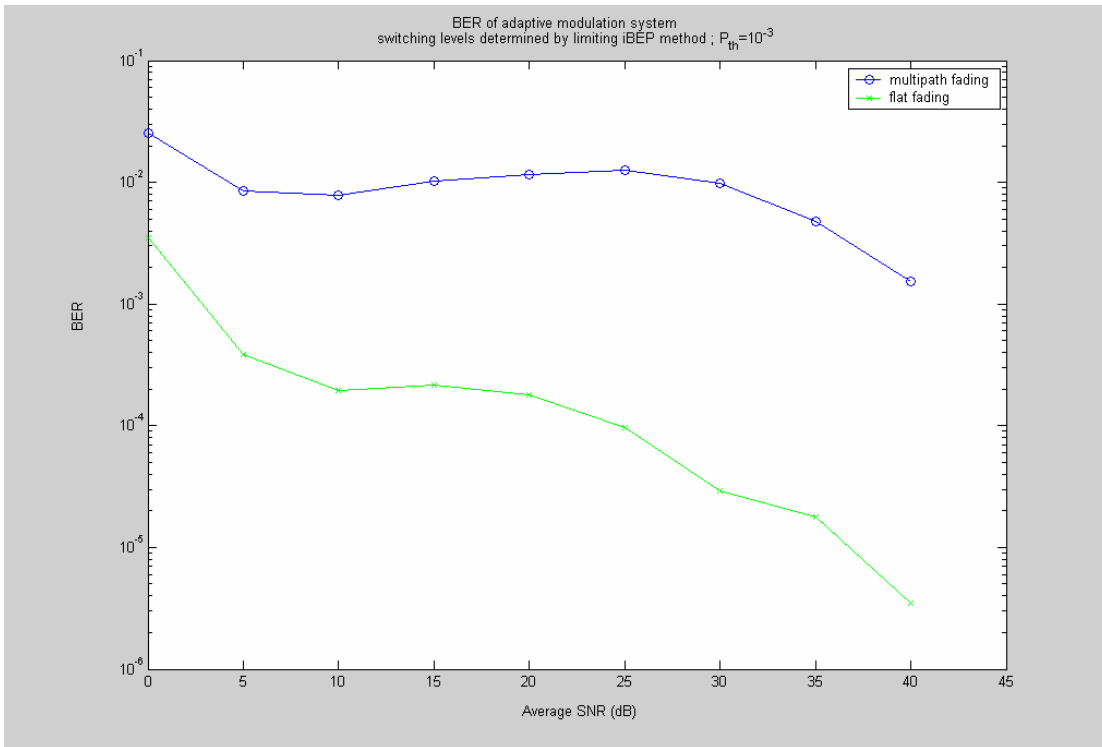| burst profile parameter	
Modulation type	No transmission, BPSK, QPSK, 16-QAM, 64-QAM
Preamble length	length=mU symbols; $m = 3,5,10$ repeated UWs;
Unique Word length	$U = 64$ symbols
Pilot Word parameters	$n = 1$ repeated UWs $F = 256$ symbol interval

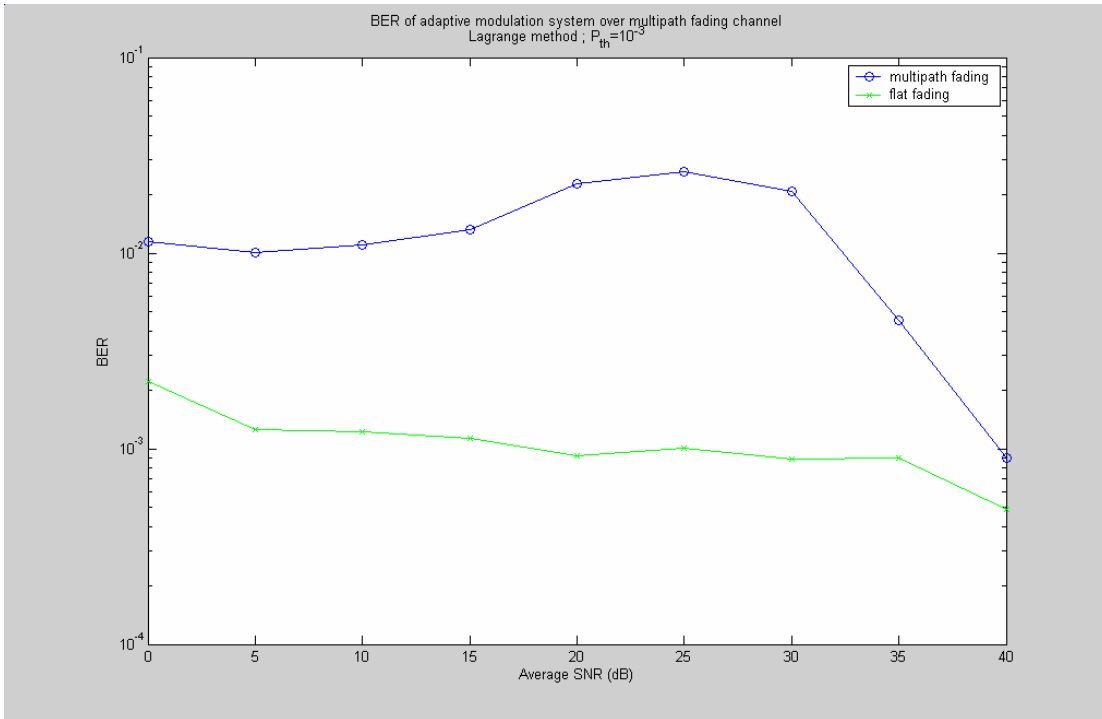Figure 4.17 (a): BER of adaptive modulation system; limiting iBEP

at $P_{th} = 10^{-3}$

Figure 4.17 (b): BER of adaptive modulation system; Lagrange method;
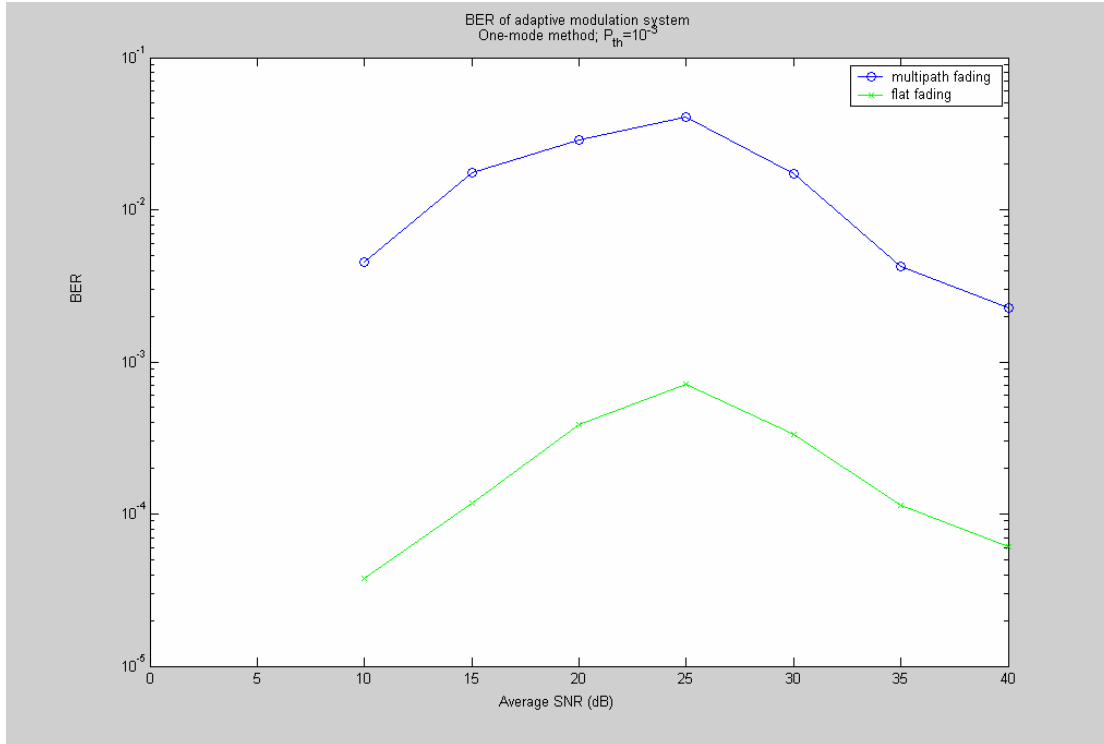
$P_{th} = 10^{-3}$

Figure 4.17 (c): BER of adaptive modulation system; One-mode method

$$P_{th} = 10^{-3}$$

As the counterpart of limiting iBEP method in the flat fading channel case, the switching levels for frequency selective fading channel can be selected as those making the average iBEP equals to the target BER. The BER of fix-mode modulation for various instantaneous SNR are shown in Fig. 4.18. Note that for the same instantaneous SNR, there may be different channel impulse response in frequency selective fading channel case and thus different BER may occur. So the BER in Fig. 4.18 are averaged values over possible conditions. From the figure, we also can observe the effect of the number of training blocks N. $N = 2$ and 10 ($m = 3$ and 11) correspond to the minimum and maximum allowable number in 802.16 SCa. It can be seen that number of training blocks N plays more important role as the more robust modulation mode are considered. For the four modulation schemes,

$N = 4$ almost approximate the performance of $N = 10$. Thus for most of our simulations for multipath fading condition, N is chosen as four.
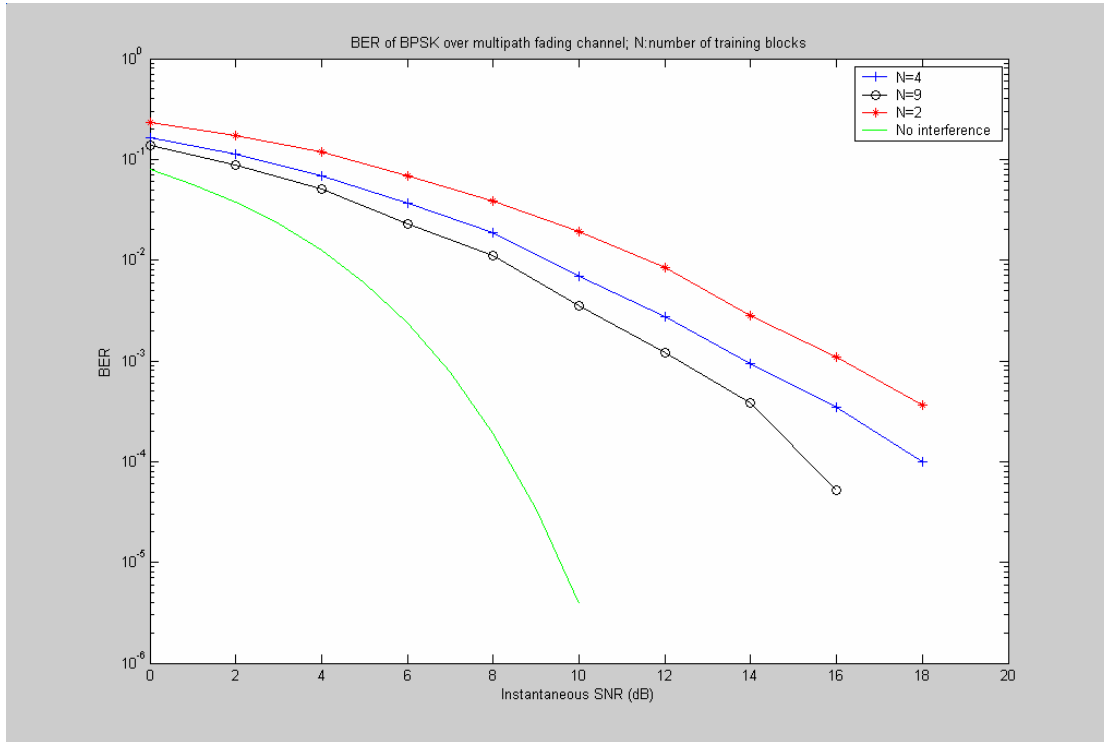

Figure 4.18(a): BER of BPSK over frequency selective fading channel.
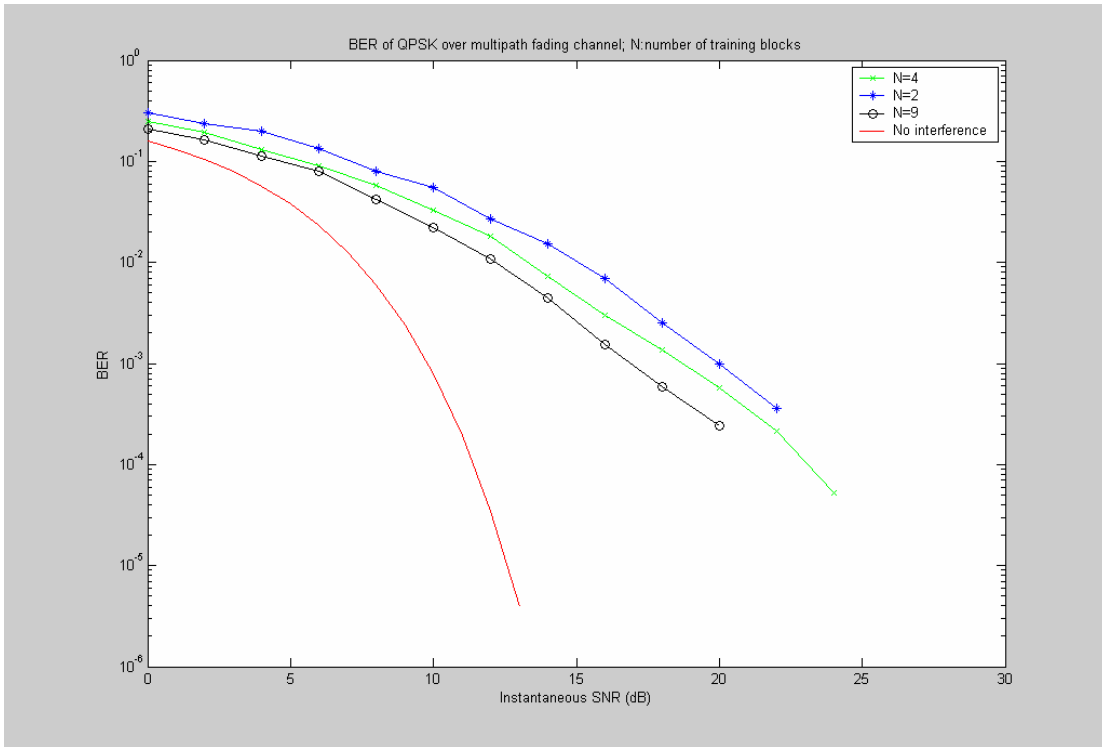
Figure 4.18(b): BER of QPSK over frequency selective fading channel.
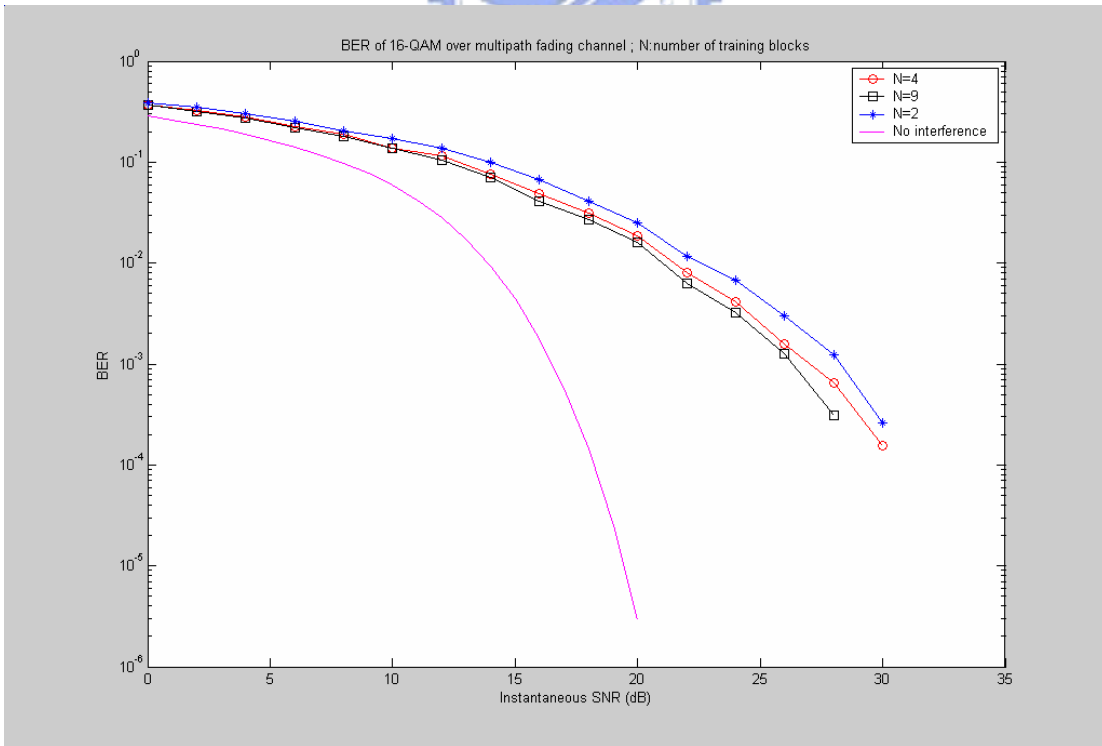

Figure 4.18(c): BER of 16-QAM over frequency selective fading channel.
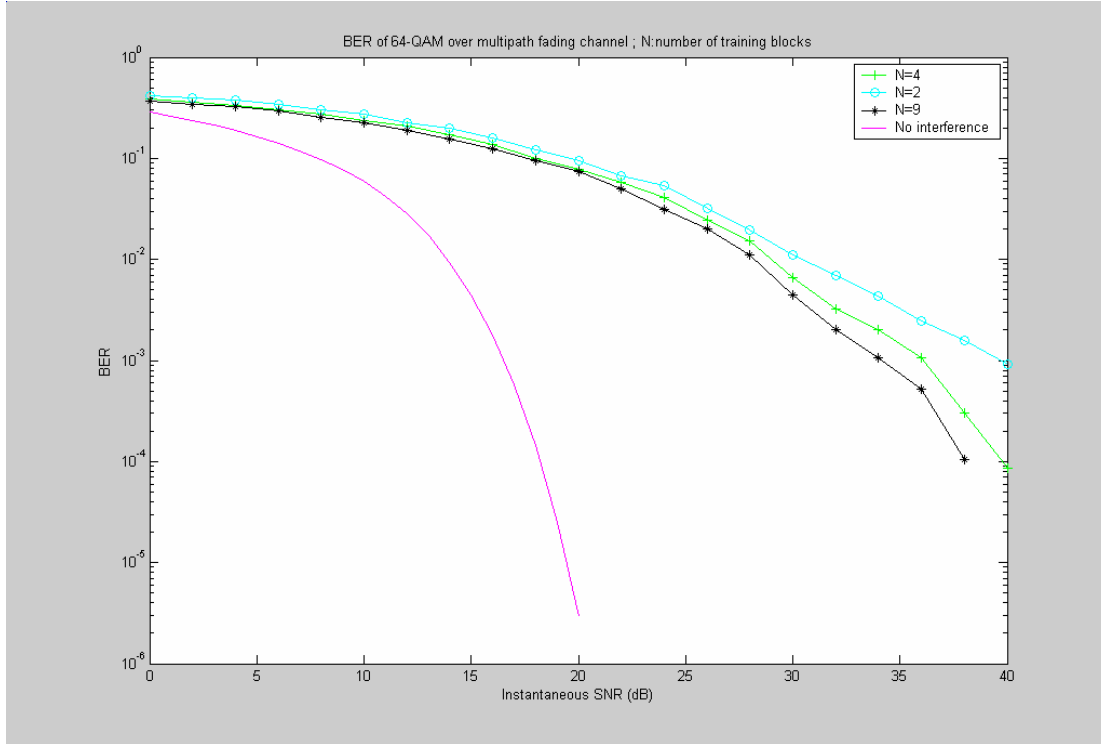
Figure 4.18(d): BER of 64-QAM over frequency selective fading channel.

Now applying the same concept of limiting iBEP method in flat fading to multipath fading condition, the switching levels assuring average iBEP below some target P_{th} are determined by:

$$S = \{s_k \mid \text{BER}_k(s_k) = P_{th}, \forall k \geq 1\} \qquad (4.4)$$

where BER_k is BER of mode-k modulation in multipath fading channel. The switching levels derived for $P_{th} = 10^{-3}$ and 10^{-2} from equation 4.4 are listed in Table 4.3. The differences between the flat fading and frequency selective fading conditions are also shown. The differences represent the SNR increment needed for the fixed modulation schemes to achieve the same BER in frequency selective fading channel as in flat fading channel around the target BER. Since a well-designed adaptive modulation system always operate around the target BER, the other switching levels derived by advanced methods in chapter 2 can be modified by adding this SNR

increment and then used for multipath fading channel.

Table 4.3 (a): switching levels at $P_{th} = 10^{-3}$

	flat	Frequency selective	difference
s1	6.8	14	7.2
s2	9.8	18	8.2
s3	16.5	27	10.5
s4	22.5	36	13.5

Table 4.3 (b): switching levels at $P_{th} = 10^{-2}$

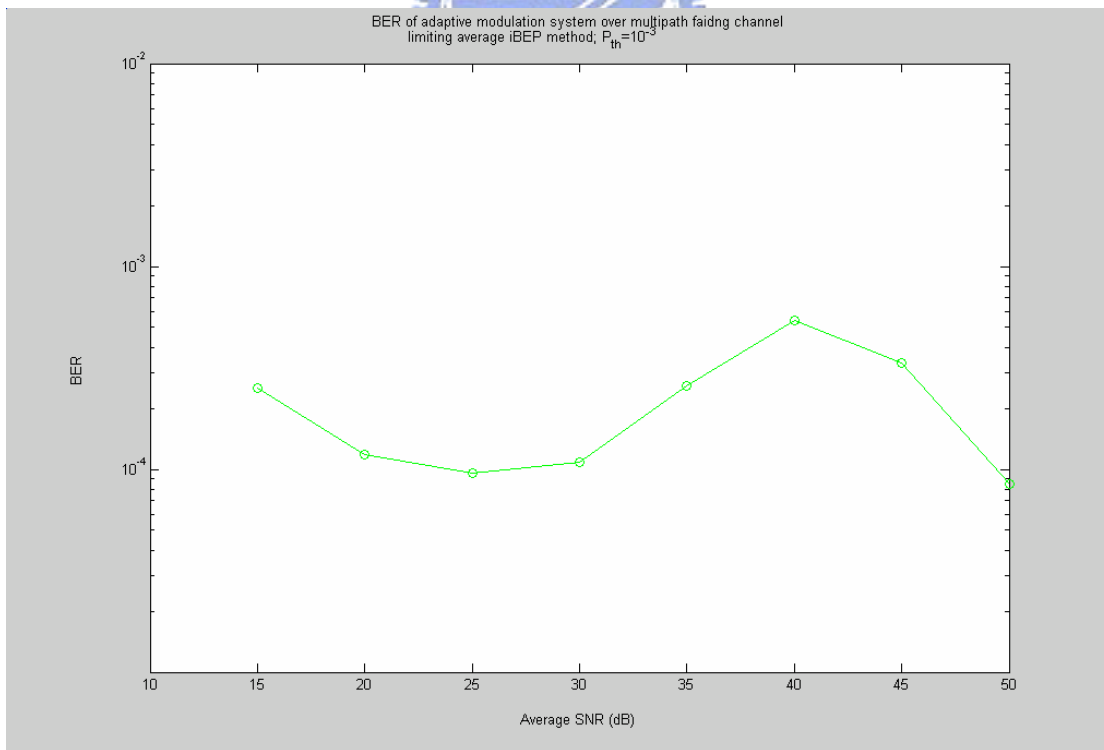|	flat	Frequency selective	difference
s1	4.3	9	4.7
s2	7.3	14	6.7
s3	13.9	22	8.1
s4	19.7	30	10.3

Figure 4.19 (a): BER of adaptive modulation system over multipath fading channel; limiting iBEP method; $P_{th} = 10^{-3}$
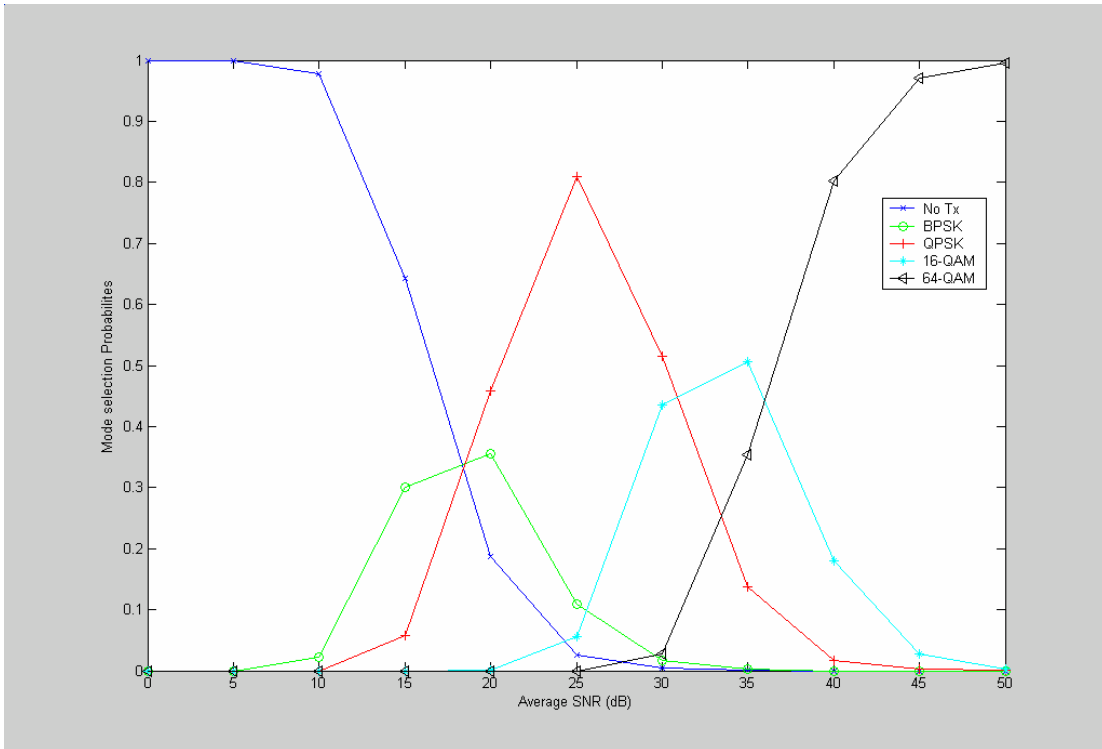
Figure 4.19 (b): Mode selection probability of adaptive modulation system
over multipath fading channel; limiting iBEP
method; $P_{th} = 10^{-3}$

Fig. 4.19 shows the BER and mode-selection-probability of the adaptive modulation system using limiting average iBEP method over multipath fading channel. Over most of the average SNR, the BER is in the range between 10^{-3} and 10^{-5}. When average SNR is larger than 45dB, almost at all time 64QAM is used and the BER approaches that of fix-64QAM system and decreases as SNR increases. Fig. 4.20 shows BER and mode-selection-probability using modified One-mode and Lagrange methods. The modified Lagrange switching levels are too optimistic to result in an excessive BER between 30 and 40dB. Fig. 4.21 shows BPS performance of the three methods. BPS of modified one-mode method outperforms that of limiting average iBEP method for average SNR larger

than 20dB. It is because that switching levels of limiting iBEP method don't adjust to different average SNR condition and thus too conservative when average SNR is high, same reason as in flat fading case.
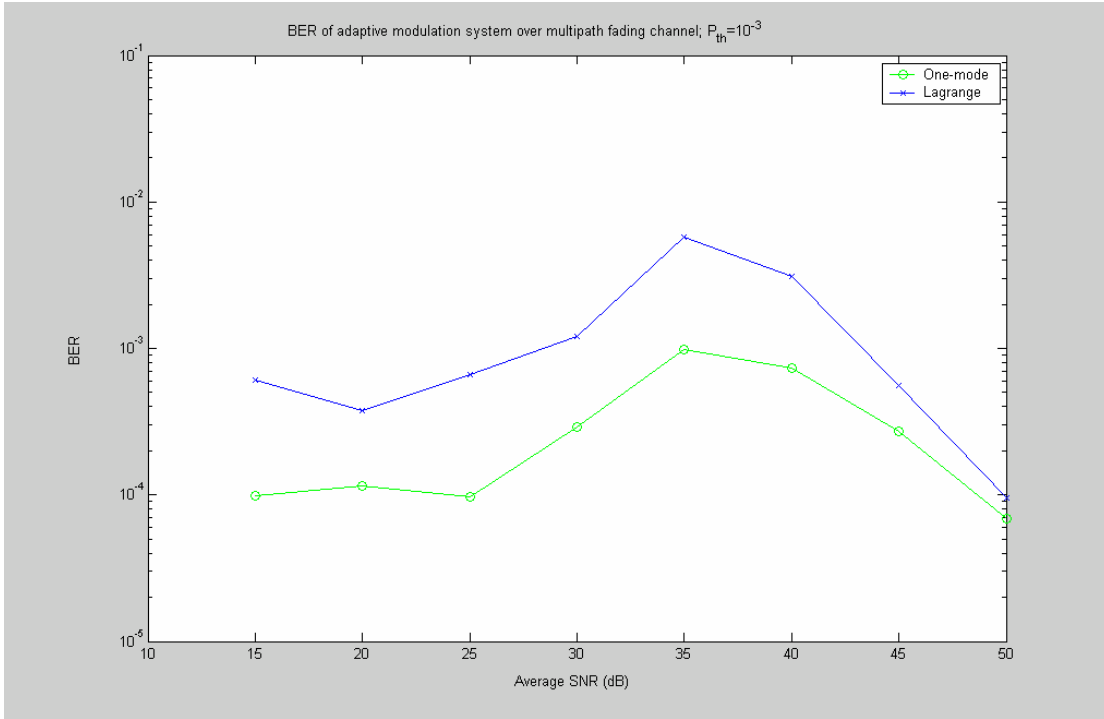

Figure 4.20 (a): BER of adaptive modulation system over multipath fading channel; $P_{th} = 10^{-3}$
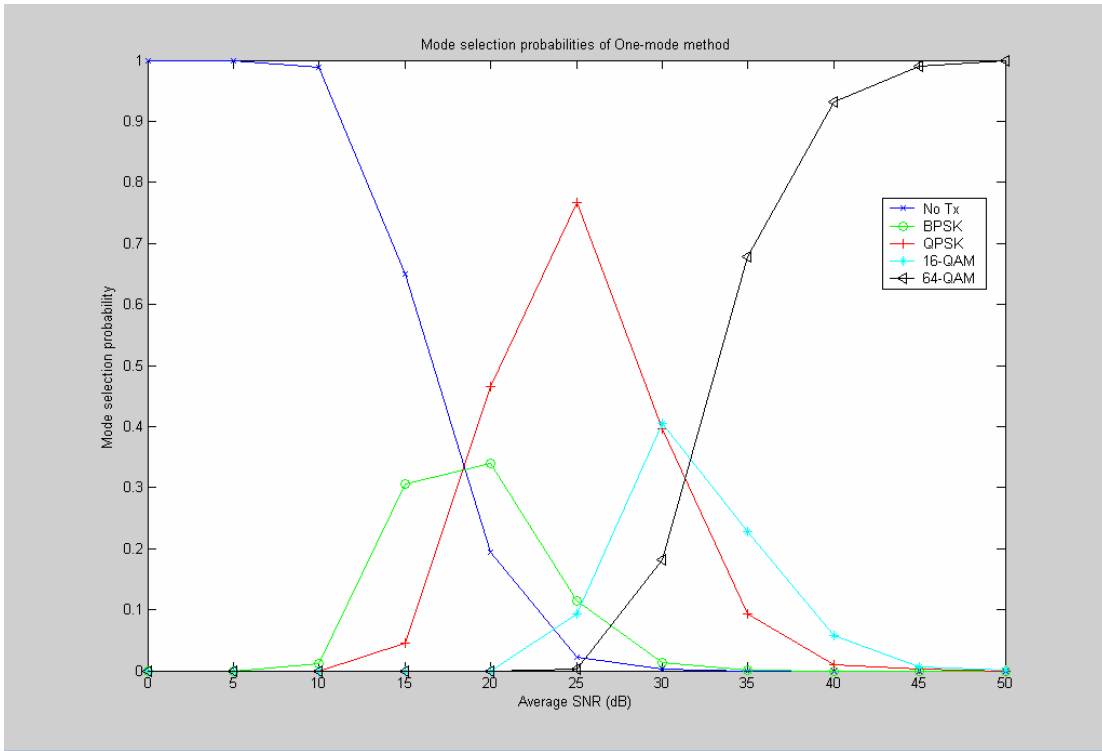
Figure 4.20 (b): Mode selection probability of adaptive modulation system over multipath fading channel; One-mode method; $P_{th} = 10^{-3}$
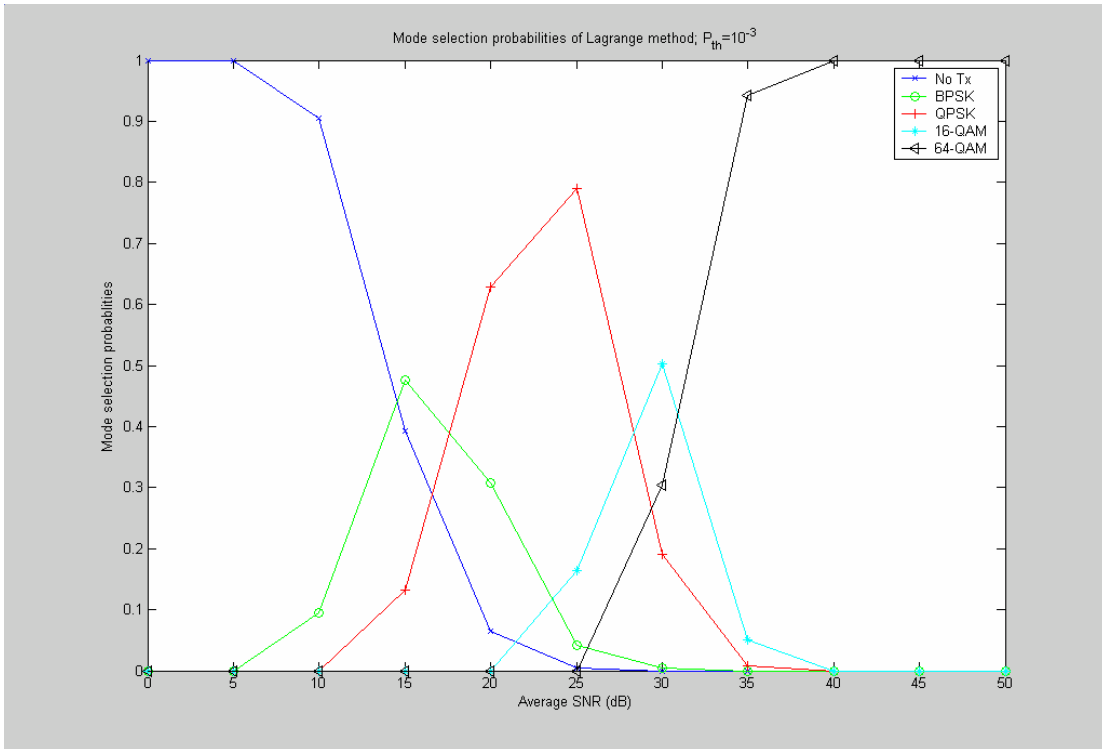
Figure 4.20 (c): Mode selection probability of adaptive modulation system over multipath fading channel; Lagrange method; $P_{th} = 10^{-3}$
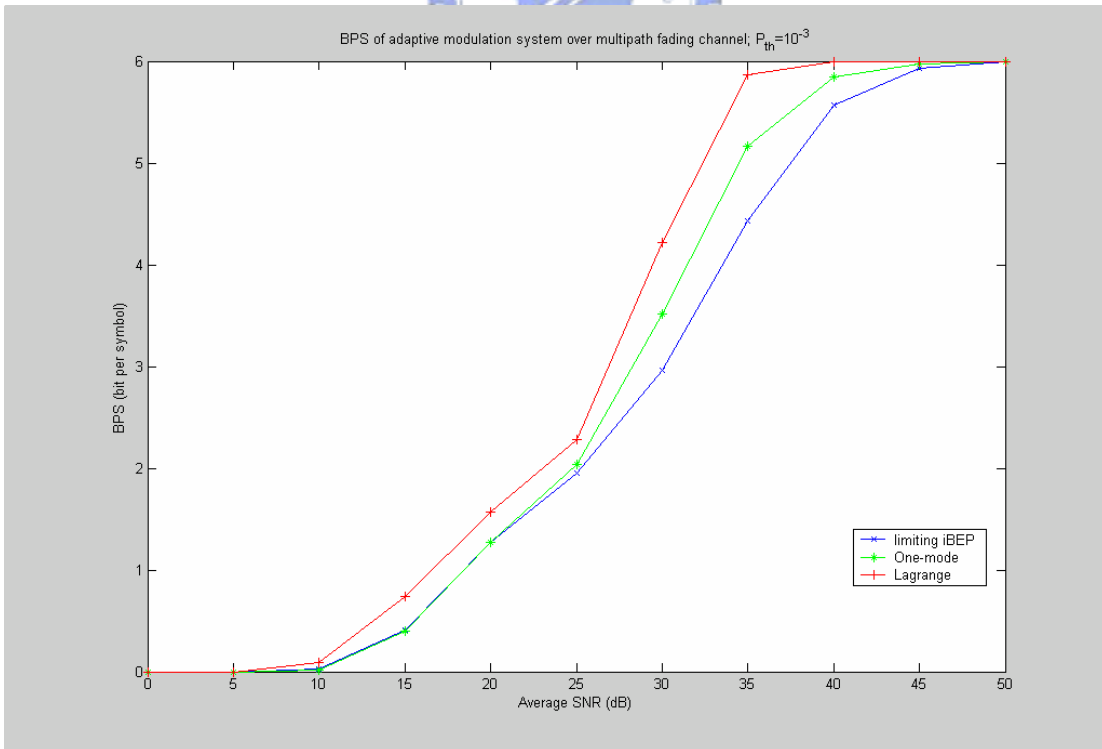

Figure 4.21: BPS of adaptive modulation systems over multipath fading channel at $P_{th} = 10^{-3}$

Chapter 5

Conclusion

_____

Adaptive modulation is a useful technique to improve the bandwidth
efficiency and increase the data rate over a fading channel. Modulation
mode selection is critical in an adaptive modulation system. Several methods
to determine the switching levels for flat fading channel are introduced in
chapter 2.

The BER of non-adaptive QAM over a multipath fading channel
depends on channel characteristic and equalizer techniques. Thus the
switching levels can't be calculated analytic as in flat fading condition. In
chapter 4, the performance degradation due to multipath fading effect is
simulated and used to adjust the switching levels to the multipath fading
channel. Similar mechanism can be repeated for other practical system, no
matter any fading channel characteristics and any equalizer type.

Appendix A

Equalizer Training using Least Square Minimization for Frequency domain DFE

Consider the block diagram of FD-DFE in Fig. 4.5. The training procedure tries to determine the equalizer coefficients based on the least-square (LS) optimization during the reception of N consecutive training blocks. Each training block consists of a sequence of P known transmitted training symbols $\{a_k, k = 0, 1, ... P-1\}$. Assuming that for each block, same sequence is transmitted. P has to be set to at least equal to the maximum expected channel impulse response length. If $P < M$, where M is length of data payload block, the forward filter parameters derived from training, $\{\tilde{W}_l, l = 0, 1, ... P\}$ can be interpolated to values to be used for a length-M data block.

The error at the mth sample of the nth training block can be expressed as:

$$
\begin{aligned}
e_m^{(n)} &= z_m^{(n)} - a_m^{(n)} \\
&= \frac{1}{P} \sum_{l=0}^{P-1} \left[\tilde{W}_{l+kP} R_{l+kP}^{(n)} \right] \exp(j \frac{2\pi}{P} lm) - \sum_{k \in F_B} \tilde{f}_k^* a_{m-k} - a_m
\end{aligned}
\tag{A.1}
$$

where $m = 0, 1, 2, ...(P-1); n = 1, 2, ...N$.

Let $\{R_l\}, \{A_l\}$, and $\{H_l\}$ are FFT of $\{r_m\}, \{a_m\}$, and $\{h_m\}$. Let the operation $\langle X \rangle = \frac{1}{N} \sum_{n=1}^{N} X^{(n)}$, and then we can write the sum of squared errors that is to be minimized as:

$$\sum_{m=0}^{P-1}\left\langle\left|e_m^{(n)}\right|^2\right\rangle=\frac{1}{P}\sum_{l=0}^{P-1}|A_l|^2\,\tilde{W}_l^H\tilde{U}_l\tilde{W}_l-\frac{2}{P}\mathrm{Re}[\sum_{l=0}^{P-1}|A_l|^2\,\tilde{W}_l^H\tilde{H}_l^*F_l]+\frac{1}{P}\sum_{l=0}^{P-1}|A_l|^2\,|\tilde{F}_l|^2 \qquad (A.2)$$

where superscript H means complex conjugate transpose, and

$$\tilde{U}_l=\left\langle\frac{R_lR_l^H}{|A_l|^2}\right\rangle,\ \tilde{H}_l=\left\langle\frac{R_l}{A_l}\right\rangle,\ \text{and}\ \tilde{F}_l=1+\sum_{k\in F_B}\tilde{f}_k^*\exp(-j2\pi\frac{lk}{P})$$

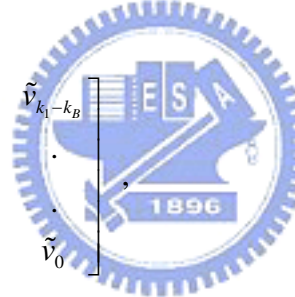Minimizing the sum of squared errors with respect to $\tilde{W}_l$ and $\tilde{f}_k$, we can get:

$$\tilde{W}_l=(\tilde{U}_l)^{-1}\tilde{H}_l^*\tilde{F}_l\ \ \text{for}\ \ l=0,1,2,...,(P-1) \qquad (A.3)$$

and

$$\tilde{\mathbf{f}}=(\tilde{f}_{k_1},\tilde{f}_{k_2},....,\tilde{f}_{k_B})=-\tilde{\mathbf{V}}^{-1}\tilde{\mathbf{v}} \qquad (A.4)$$

where
$$\tilde{\mathbf{v}}=(\tilde{v}_{k_1},\tilde{v}_{k_2},...\tilde{v}_{k_B})'\ ,$$

$$\tilde{\mathbf{V}}=\begin{bmatrix}\tilde{v}_0 & \tilde{v}_{k_1-k_2} & \cdots & \tilde{v}_{k_1-k_B}\\ \tilde{v}_{k_2-k_1} & \tilde{v}_0 & \cdot & \cdot\\ \vdots & \cdot & \ddots & \cdot\\ \tilde{v}_{k_B-k_1} & \cdot & \cdot & \tilde{v}_0\end{bmatrix},$$

$$\tilde{v}_k=\sum_{l=0}^{F-1}|A_l|^2\left[1-|\tilde{H}_l|^2\tilde{U}_l^{-1}\right]\exp(-j2\pi\frac{lk}{P})$$

$$\qquad (A.5)$$

What next to do is interpolating the P forward equalizer coefficients to M coefficients. First compute the inverse FFT, of length P, of each component of the vector $\dfrac{\mathrm{R}_l^{(n)}}{A_l}$. Then pad the resulting sequences with zeroes to length M. After taking FFT, the final version of $\dfrac{\mathrm{R}_l^{(n)}}{A_l}$ is of length M and used to compute $\tilde{H}_l$ and $\tilde{U}_l$.

Bibliography

[1] Theodore, S. Rappaport, *Wireless Communications: principles and practice*, second edition, Prentice Hall, 1996

[2] L. Hanzo, C. H. Wong, and M. S. Yee, *Adaptive wireless transceivers,* Wiley,2002

[3] B.-J. Choi, and L. Hanzo, "Optimum mode-switching assisted adaptive modulation," in Proc. IEEE GLOBECOM '01, San Antonio, TX USA, Nov. 2001, vol.6, pp. 3316-3320

[4] John. G. Proakis, *Digital communications*, fourth edition, McGraw-Hill, 2000

[5] D. Yoon, K. Cho, and J. Lee, "Bit error probability of M-ary Quadrature Amplitude Modulation" in Proc. IEEE VTC 2000-Fall, vol. 5. pp 2422-2428, IEEE Setember 2000

[6] W. T. Webb and R. Steele, "Variable rate QAM for mobile radio," IEEE Trans. Commu., vol. 43, no. 7, pp. 2223-2230, July 1995.

[7] IEEE Std 802.16-2001, *IEEE Standard for Local and Metropolitan Area Networks – Part 16: Air interface for Fixed Broadband Wireless Access Systems*. New York: IEEE, April 2, 2002.

[8] *http://www.wirelessman.org/pub/backgrounder.html*

[9] IEEE Std 802.16a-2003, *IEEE Standard for Local and Metropolitan Area Networks – Part 16: Air interface for Fixed Broadband Wireless Access Systems – Amendment 2: Medium Access Control Modifications and Additional Physical Layer Specifications for 2-11 GHz.* New York: IEEE, April 1, 2003.

[10] D. Falconer, S. L. Ariyavisitakul, A. Benyamin-Seeyar, and B. Eidson, "Frequency domain equalization for single-carrier broadband wireless systems," *IEEE Commun. Mag*., vol. 40, no. 4, pp. 58-66, Apr. 2002.

[11] J. Torrance and L. Hanzo, "Optimization of switching levels for

adaptive modulation in a slow Rayleigh fading channel", Electronics Letters, vol. 32, pp 1167-1169, 20 June 1996

[12] A. Goldsmith and S. Chua, "Variable rate variable power MQAM for fading channels", IEEE transactions on Communications, vol. 45, pp. 1219-1230, October 1997

[13] M. S. Alouini and A. Goldsmith, "Capacity of fading channels with channel side information", IEEE transaction on Information Theory, vol 43, pp 1986-1992, Noverber 1997

[14] S. Otsuki, S. Sampei, and N. Morinaga, "Square QAM adaptive modulation/TDMA/TDD systems using modulation level estimation with Walsh function", Electronic Letters, vol. 31 pp 169-171

[15] J. Torrance and L. Hanzo, "Demodulation level selection in adaptive modulation," Electronics Letters, vol.32 pp 1751-1752, September 1996

[16] J. K. Cavers, "Variable rate transmission for Rayleigh Fading channels", IEEE Transactions on Communication Technology, vol. COM-20, pp 15-22 February 1972

[17] R. Steele and W. Webb, "Variable rate QAM for data transmission over Rayleigh fading channels" in Proceedings of Wireless '91, pp 1-14, IEEE 1991

[18] V. Erceg et. Al. "Channel models for Fixed Wireless Applications", IEEE 802.16.3c-01/29r1